6-2018

The Role of Wnt3a in Ischemic Stroke

Nathanael Matei

LOMA LINDA UNIVERSITY
School of Medicine
in conjunction with the
Faculty of Graduate Studies

The Role of Wnt3a in Ischemic Stroke

by

Nathanael Matei

A Dissertation submitted in partial satisfaction of
the requirements for the degree
Doctor of Philosophy in Biochemistry

June 2018

Each person whose signature appears below certifies that this dissertation in his/her opinion is adequate, in scope and quality, as a dissertation for the degree Doctor of Philosophy.

_____, Chairperson
John H. Zhang, Professor of Neurosurgery, Neurology, Physiology, and Anesthesiology

_____
Ravi Goyal, Associate Professor of Pharmacology

_____
Salma Khan, Assistant Professor of Biochemistry

_____
Christopher Perry, Assistant Professor of Biochemistry

_____
Jiping Tang, Professor of Physiology and Pharmacology

ACKNOWLEDGEMENTS

The path toward this dissertation has been one of perseverance. Its completion is thanks to the special people who challenged, supported, and assisted me throughout the years.

First, I would like to express my deepest gratitude to Dr. John H Zhang, Phd Mentor, for giving me the opportunity to carry out my research in his neuroscience lab at Loma Linda University. Dr. Zhang has given me constant guidance, encouragement, and the necessary training to succeed as a principal investigator.

I would also like to express my deepest thanks and sincere appreciation to my committee members and lab-mates for their contributions to my work.

My utmost gratitude and appreciation go to Dr. Lawrence Longo for taking a shot on me and opening the first door to my PhD career. Although he is no longer with us today, I hope to make him proud with my future work in medical research, and as he always stated, “Persevere!”

To my family, friends, and church, your love and encouragement has sustained me during this challenging process to pursue my dream.

And finally, I would like to thank God for providing me the unmerited opportunity to study His creation and marvel at its complexity.

CONTENTS

FIGURES

Figures Page

Chapter 1

Chapter 2

TABLES

Tables Page

ABBREVIATIONS

LD	Low Dose (0.4 µg/kg)
HD	High Dose (1.2 µg/kg)
FRZ1	Frizzled-1
MCAO	Middle Cerebral Artery Occlusion
rtPA	Recombinant Tissue Plasminogen Activator
BBB	Blood Brain Barrier
CNS	Central Nervous System
LRP5/6	Lipoprotein receptor related proteins 5 and 6
CC-3	Cleaved Caspase-3
CRISPR	Clustered Regularly Interspaced Short Palindromic Repeats

ABSTRACT OF THE DISSERTATION

The Role of Wnt3a in Ischemic Stroke

by

Nathanael Matei

Doctor of Philosophy, Graduate Program in Biochemistry
Loma Linda University, June 2018
Dr. John H. Zhang, Chairperson

After ischemic stroke, apoptosis of neurons is a primary factor in determining outcome. Wnt3a is a naturally occurring protein that has been shown to have protective effects in the brain for traumatic brain injury. Although wnt3a has been investigated in the phenomena of neurogenesis, anti-apoptosis, and anti-inflammation, it has never been investigated as a therapy for stroke. We hypothesized that the potential neuroprotective agent wnt3a would reduce infarction and improve behavior following ischemic stroke by attenuating neuronal apoptosis and promoting cell survival through the Frizzled-1/PIWI1a/FOXM1 pathway in MCAO rats. 229 Sprague-Dawley rats were assigned to male, female, and aged 9-month male MCAO or sham groups followed by reperfusion 2 hours after MCAO. Animals assigned to MCAO were either given wnt3a or its control. To explore the downstream signaling of wnt3a, the following interventions were given: Frizzled-1 siRNA, PIWI1a siRNA, and PIWI1a-CRISPR, along with the appropriate controls. Post-MCAO assessments included neurobehavioral tests, infarct volume, Western blot, and immunohistochemistry. Endogenous levels of wnt3a, Frizzled-1/PIWI1a/FOXM1, were lowered after MCAO. The administration of intranasal wnt3a, 1 h post MCAO, increased PIWIL1a and FOXM1 expression through Frizzled-1, reducing brain infarction and neurological deficits at 24 and 72 hours. Frizzled-1 and

PIWI1a siRNAs reversed the protective effects of wnt3a post MCAO. Restoration of PIWIL1a after knockdown of Frizzled-1 increased FOXM1 survival protein and reduced Cleaved Caspase-3 levels. In summary, wnt3a decreases neuronal apoptosis and improves neurological deficits through Frizzled-1/PIWI1a/FOXM1 pathway after MCAO in rats. Therefore, wnt3a is a novel intranasal approach to decrease apoptosis after stroke.

CHAPTER ONE

THE ROLE OF APOPTOSIS IN ISCHEMIC STROKE

Nathanael Matei[1]

Department of [1]Physiology, Loma Linda University, Loma Linda, California 92354

Note: Most of this chapter is taken from a review paper currently in the submission process.

Introduction

What is Stroke

Stroke is the rapid development of disturbance of cerebral function attributed to the interrupted blood supply lasting longer than 24 hours. The two main types of stroke are ischemic and hemorrhagic, with incidences accounting for 85% and 15% respectively (Musuka et al., 2015). Ischemic stroke is the 3rd leading cause of mortality globally and the number one cause of disability. The incidence of stroke increases exponentially with age, with a 100-fold increase in rates between the 3rd and 4th decades and the 8th and 9th decades (Bonita, 1992). More than a third of stroke cost is due to lost productivity rather than actual treatment (Mackay and Mensah, 2004).

Due to the plethora of causes for Ischemic stroke, syndrome characterization occurs by a rule of quarters: 25% cardioembolic, 25% arteroembolic, 25% lacunar, and 25% due to other causes (Ay et al., 2005). Of note, the majority of acute coronary syndromes result from a rupture or erosion of an atherosclerotic plaque, followed by in situ formation of a thrombus on the plaque, causing arterial obstruction (DeWood et al., 1980). Normally, ischemic stroke occurs from embolic arterial occlusion—either cardioembolic, caused by atrial fibrillation or valvular heart disease, or arteroembolic, from atherosclerotic disease in the extracranial cervical carotid or vertebral artery (Musuka et al., 2015). Cerebral blood flow through collateral vessels, near the embolic arterial occlusion, may help prevent total ischemia and ameliorate hypoxia-induced damage; however, it remains inefficient in maintaining neuronal function and viability at the infarct core (Ay et al., 2005). With anaerobic conditions, complex metabolic events result in irreversible damage and neuronal death (Lott et al., 1999).

Stroke Pathophysiology

In the acute stage of oxygen and glucose depletion in the brain, decreased blood flow disrupts ionic homeostasis, increasing intracellular calcium stress responses, which releases excitatory neurotransmitters and induces mitochondrial dysfunction, leading to increased reactive oxygen species (ROS) generation (Kurisu and Yenari, 2017). In the sub-acute stage, hours to days later, apoptotic and inflammatory pathways are initiated, leading to neuronal cell death. Additionally, the increase in ROS and cytokines results in blood brain barrier deterioration, enabling protein and water to flood into the extracellular space, leading to vasogenic edema (Sun et al., 2015). The labyrinth of sub-acute stroke induced pathways include apoptosis, excitotoxicity, inflammation, and oxidative stress.

In the recent pharmacological developments for stroke, attenuation of microcirculatory disturbances has been targeted by ablating single factors in the pathogenesis, including recombinant tissue plasminogen activator (rtPA), antioxidants, anti-intercellular adhesion molecule-1 (ICAM-1) antibody, calcium-stabilizing agents, and anti-excitotoxic agents (Sun et al., 2015). Hitherto, rtPA continues to be the only FDA approved pharmacological intervention approved for acute ischemic stroke despite multiple clinical trial exploring alternative treatments (Roth, 2011). Although FDA approved, rtPA is not without side effects, and even when administered as indicated, rtPA causes a 5.8% increase in the incidence of symptomatic hemorrhagic transformation (Horn et al., 1998). With the lack of effective treatments, novel therapies may change the clinical management of Stroke patients and provide a foundation for future research in other types of strokes with similar pathologies. Blood brain barrier damage,

inflammation, and apoptosis all contribute to the poor outcomes in ischemic stroke (Broughton et al., 2009; Jin et al., 2010; Leigh et al., 2014).

Apoptosis

With the loss of oxygen and glucose, a hypoxic state is created in the acute stage of cerebral infarction, and recanalization causes a stress response, triggering neuronal cell apoptosis and loss of biological function (Candelario-Jalil, 2009). A major contributor to outcome after stroke is the survival of neurons (Lai *et al.*, 2014). Thus, a major therapeutic target for the treatment of stroke has been protection of neurons (Cerpa *et al.*, 2009; Lai *et al.*, 2014). Of particular interest, studies have reported the activation of extrinsic and intrinsic pathways of caspase-mediated cell death in several forms of transient MCAO in adult rats (Ferrer & Planas, 2003). Stress-induced signaling events cause damage to DNA, cellular structures, and organelles—including cytoskeleton, mitotic microtubules, mitochondria, golgi, and sarcoplasmic reticulum(López-Hernández et al., 2006).

Intrinsic pathways are activated when the mitochondria is damaged, causing membrane depolarization and permeabilization, and subsequently releasing several proapoptotic factors from the mitochondrial space (Ferri and Kroemer, 2001). When Cytochrome c is released, due to mitochondrial damage, binding occurs between cytosolic apaf-1 and procaspse 9 in a dATP-dependent manner to form the apoptosome, resulting in the autoproteolytic activation of caspase 9 (López-Hernández et al., 2006). Next, caspase 9 cleaves downstream effector caspases, 3, 6 and 7, phenotypic markers of apoptosis (Le et al., 2002; Shabanzadeh et al., 2015). Cleaved-caspase-3 is upregulated

following MCAO, and subsequently, the inhibition of caspase-3 reduces infarct size following transient MCAO (Ferrer & Planas, 2003). Thus, our hypothesis is that attenuation of cleaved-caspase-3 and prevention of neuronal apoptosis will provide therapeutic benefits following ischemic stroke in rats.

Effect of Sex on Stroke

The epidemiology of ischemic stroke is sexually dimorphic, and therapeutic agents vary in male and female subjects. Prevalence of ischemic stroke is higher in men of all age cohorts, though the significance lessens between sexes after the age of 75 years (Peisker et al., 2017). Prior to menopause, women exhibit a lower risk of stroke compared to their age-matched men, but after menopause this effect diminished, increasing the incidence of stroke in women (Liu and McCullough, 2011). Estradiol has neurotrophic, antiapoptotic, vasodilatory, anti-inflammatory, and antioxidant effects, which has been shown to improved outcome in brain ischemic models of males and females (McCullough and Hurn, 2003). However, the Woman's Health Initiative, a clinical trial of Estradiol replacement for stroke prevention, showed an increase in stroke incidence in estrogen-treated women.

Prevention

Given the lack of treatments, prevention is key to reduce stroke onset. Important modifiable risk factors for stroke prevention include high blood pressure, atrial fibrillation, high blood cholesterol levels, diabetes mellitus, cigarette smoking, heavy alcohol use, drug use, lack of physical activity, obesity, and unhealthy diet (Anon, 1985;

Sacco et al., 1997; Hankey, 1999). The dearth of effective treatments for a disease with such significant morbidity, mortality, and socioeconomic consequences and the failure of all pharmacological trials, with the exception of rtPA, is evidence for the need to develop novel therapies that target other potential contributors to poor outcomes following ischemic stroke.

Specific Aims

The specific aims are to: Evaluate the neuroprotective effect of intranasal (iN) wnt3a administration after middle cerebral artery occlusion model in rats. **Our main hypothesis is that MCAO will decrease the levels of wnt3a expression in the brain and administering iN wnt3a will provide beneficial effects**. Animal models of ischemic stroke have shown an increased neuronal apoptosis following ischemic injury and higher expression of caspase-3 in animal models (Chacón et al., 2008; Shruster et al., 2012; Arrázola et al., 2015). We suggest that decreased activation of Frz-1, due to lower levels of circulating wnt3a following ischemic stroke, will increase neuronal apoptosis. Wnt3a has been shown to upregulate PIWIL1a (Reeves et al., 2012) and FoxM1 (Zhang et al., 2011), and studies have linked FoxM1 to inhibit apoptosis (Jiang et al., 2014). Due to the dynamic stress of ischemic stroke, we will investigate the time-course expression of endogenous and exogenous wnt3a in the rat brain (Aim 1a), establish neuroprotective effects of the Frz1 receptor in MCAO (Aim 1b), determine the role of wnt3a in sham and MCAO rats by inhibiting wnt3a (Aim 1c), determine the best treatment regimen for wnt3a administration (Aim 1d), determine cell expression of Frz1 in the brain (Aim 1e), evaluate the sexual dimorphism in male and female rats after MCAO and treated with

wnt3a (Aim 1f), determine the age-related differences in young versus old MCAO rats (Aim 1g), and evaluate a permanent occlusion model (Aim 1h). We expect iN wnt3a will improve neurological outcomes through reduction of neuronal apoptosis after MCAO. Aim 2 will determine the role of iN Wnt3a attenuating apoptosis via up-regulation of the Frz1/PIWIL1/FOXM1 pathway with subsequent down regulation of Caspase-3 and reduction of apoptotic neuronal cells after MCAO in rats. **Our hypothesis is that Frz1, activated by iN wnt3a, will upregulate PIWIL1a with downstream activation of FOXM1 and subsequent downregulation of Caspase-3 to reduce neuronal apoptosis after ischemic stroke.** We will investigate the effect of iN wnt3a on apoptotic neurons with Fluoro-Jade after ischemic stroke (Aim 2a), evaluate the levels of Frz1, PIWIL1a, pGSK3-β, β-catenin, FOXM1, and Caspase-3 with ischemic stroke and after treatment (Aim 2b), determine the effect of PIWIL1a inhibition and the combination of Frz1 inhibition with PIWIL1a activation to establish the wnt3a mediated anti-apoptotic effect (Aim 2c), and determine the effect of PIWIL1a activation via CRISPR after Frz1-siRNA (Aim 2d). We expect that iN wnt3a will upregulate FoxM1 and down-regulate the apoptotic GSK3-β induced intrinsic pathway; thus, sustaining neuronal survival after the post-ischemic stroke insult and improving neurobehavioral outcomes.

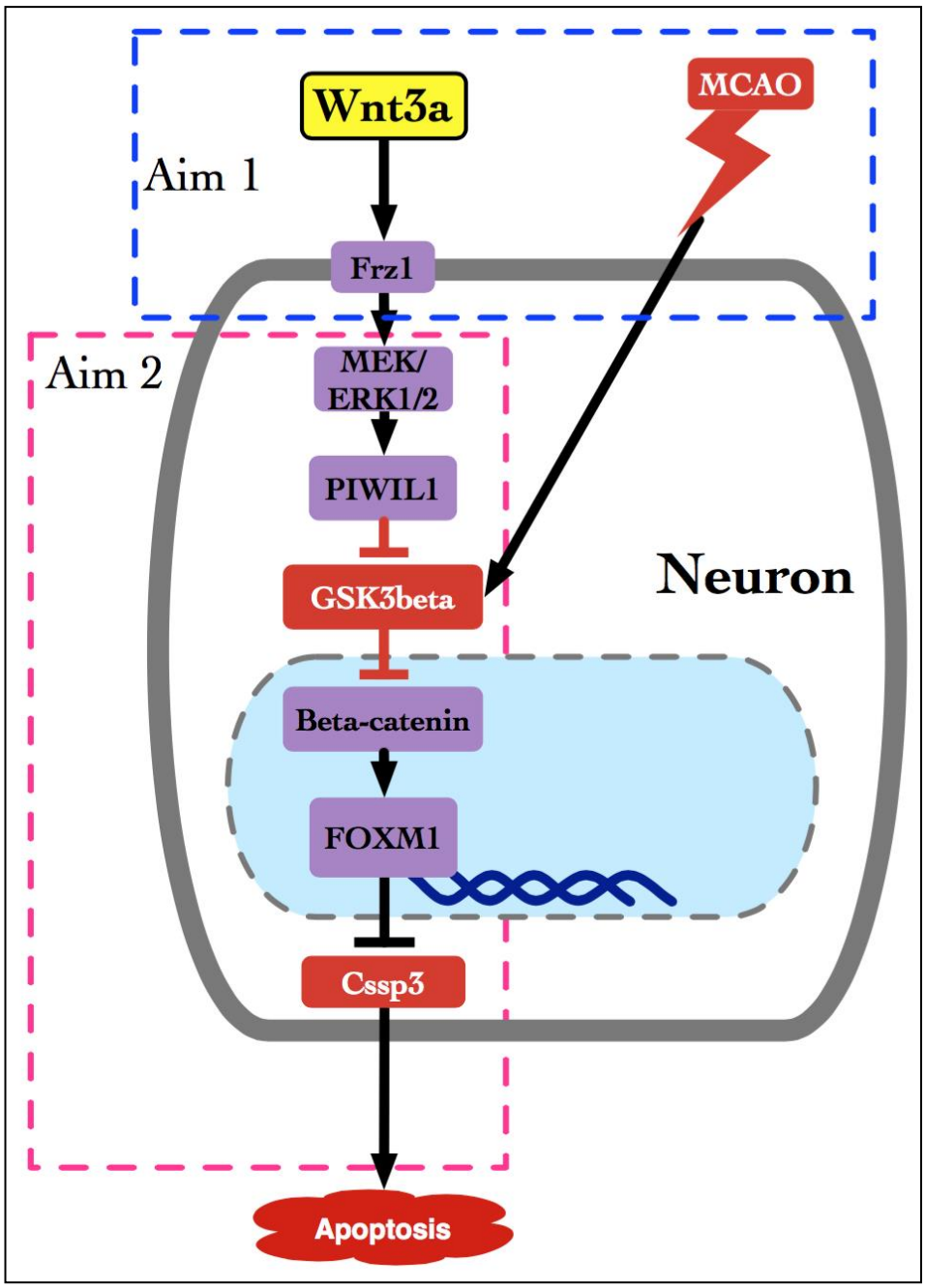

Figure 1. Proposed Aim 1 and 2 for wnt3a activation of Frizzled1 and its downstream targets. Briefly, wnt3a binds to Frizzled-1, increases PIWIL1a, inhibits the activation of GSK3β, and activates β-catenin, which translocates into the nucleus to increase the transcription of FOXM1.

Specific Aim One

Evaluate the neuroprotective effect of iN wnt3a administration after middle cerebral artery occlusion model in rats (MCAO). Our main hypothesis is that MCAO will decrease the levels of wnt3a expression in the brain and administering iN wnt3a will provide beneficial effects. Wnt3a has been shown to have protective effects in central nervous system diseases (Inestrosa and Varela-Nallar, 2014) as well as ischemic stroke (Shruster et al., 2012). To date, no studies have been done in the MCAO in-vivo stroke models to show if wnt3a may have similar advantageous effects.

Aim1a: Determine the Endogenous Levels of Frz1, PIWIL1, GSK3-β, β-catenin, FOXM1, and Caspase-3 with Ischemic Stroke

Hypothesis: MCAO in rats will decrease wnt3a-dependent activation of the Frz1→PIWIL1→β-catenin pathway with the increased expression of FoxM1.

Rationale: Animal models of ischemic stroke have shown an increase in neuronal apoptosis following ischemic injury and higher expression of caspase-3 in animal models (Chacón et al., 2008). We suggest that decreased activation of Frz-1, due to lower levels of circulating wnt3a following ischemic stroke, will increase neuronal apoptosis. Wnt3a has been shown to upregulate PIWIL1a (Reeves et al., 2012) and FoxM1(Zhang et al., 2011), and studies have linked FoxM1 to inhibit apoptosis (Jiang et al., 2014). We will do quantitative analysis with western blot of the endogenous expression of (A) wnt3a, (B) Frz1, (C) PIWIL1a, (D) pGsk-3β, (E) FOXM1 and (F) CC3. We postulate that iN wnt3a will attenuate apoptosis in neurons after ischemic stroke and that this change will be

accompanied by increased levels of molecules in Frz1→PIWIL1→β-catenin→FOXM1 pathway.

Experiments: Ischemic stroke will be induced in animals using a MCAO model. Plasma levels of wtn3a will be measured via Western blot at 6, 12, 24 and 72 hours after MCAO. Protein levels of the proposed pathway in brain samples will be measured via Western blot in sham at 24 hours after MCAO. Antibodies for wnt3a, Frz1, PIWIL1a, GSK3-β, β-catenin, FOXM1, and Caspase-3 will be used in our analysis. **Experimental Groups:** Sham, MCAO+Vehicle at 6, 12, 24, and 72 h.

Aim1b: To Establish the Neuroprotective Effects of the Frizzled-1 Receptor in Normal and MCAO Rats

Hypothesis: Inhibiting the wnt3a receptor, Frizzled-1, with siRNA, will attenuate the protective effects of Wnt3a. **Rationale**: Wnt3a can signal by binding to Frz-1 (Hendaoui et al., 2012) which is expressed in brain on neurons and microglia (Chacón et al., 2008). Activation of this receptor has been shown to be protective and cause cell survival by attenuating caspase-3 activation (Chacón et al., 2008). We expect that inhibition of Frz1 will further decrease PIWIL1, β-catenin, FOXM1, and Caspase-3.

Experiments: The Frz1 inhibitors, will be administered via ICV injection 24 hours prior to surgery. Animals will be sacrificed at 24 hours after MCAO for Western blot analysis to detect molecules involved in the Frizzled-1 dependent pathway. Western blots will be performed to measure the expression of wnt3a, Frz1, PIWIL1, GSK3-β, β-catenin, FOXM1, and Caspase-3.

Experimental Groups: Sham, MCAO+Vehicle, MCAO+wnt3a+Scrambled-siRNA, MCAO+wnt3a+Frz1asiRNA.

Aim1c: To Determine the Role of Wnt3a in Sham and MCAO Rats by Inhibiting Wnt3a

Hypothesis: Inhibiting endogenous wnt3a with siRNA, will exacerbate the effects of MCAO and increase the number of apoptotic neurons. **Rationale:** Animals models of ischemic stroke have been shown to have an increased neuronal apoptosis post-ictus, showing higher expression of cleaved caspase-3 (Chacón et al., 2008; Shruster et al., 2012). A study of wnt3a in macrophages demonstrated that cleaved caspase-3 is down-regulated with an increase of wnt3a (Arrázola et al., 2015). We suggest that decreased levels of wnt3a will result in a reduced amount of survival proteins, specifically FOXM1, and an increase in cleaved caspase-3 causing neuronal apoptosis. We expect that endogenous protection to stroke will be further weakened and neurobehavior assessments will worsen as a result of wnt3a inhibition.

Experimental Groups: Sham, MCAO+Vehicle, MCAO+wnt3a siRNA +Vehicle, MCAO+Vehicle+ endo-IWR 1 (wnt3a inhibitor). Neurobehavioral tests and mortality will be assessed at 24 and 72 hours after MCAO.

Aim1d: To Determine the Best Dosage and Route of Administration of Wnt3a and to Evaluate the Effects of iN Wnt3a Administration on Short-term and Long-term Neurological Outcomes after MCAO

Hypothesis: Since wnt3a targets important anti-apoptotic pathways, we hypothesize that iN or IP wnt3a will protect the adult rat brain as well as improve short-term and long-term behavioral outcome after ischemic stroke. **Rationale**: Brain injury associated with ischemic stroke results in sensorimotor deficits. Wnt3a signaling is initiated by binding to Frz-1 (Hendaoui et al., 2012) which is expressed in brain on neurons and microglia (Chacón et al., 2008). Activation of this receptor has been shown to be protective and cause cell survival by attenuating caspase-3 activation (Chacón et al., 2008). Qualitatively, 2.0 mm-thick slices will be stained with a redox indicator, TTC, and used to distinguish in-between metabolically active and inactive tissues. Quantitative analysis of infarct volume at 24 hours will determine the most effective dose of wnt3a**.** Long-term behavior at 72 hours will evaluate wnt3a's impact on infarction, modified Garcia, left-forelimb placement, and corner-turn. Morris water maze data and rotarod tests will be conducted at 21 to 27 days after MCAO. **Experiments and Groups**: sham, MCAO + vehicle (1h), MCAO + iN Wnt3a LD (.4ug/kg) (1h), MCAO + iN Wnt3aHD (1.2ug/kg) (1h). Neurobehavior tests will be assessed at 24h, 72h and 4 weeks to determine the efficacy of the treatment.

Aim1e: To determine the Cellular Expression of Frz1 in the Brain and How Expression Changes after Stroke via Immunohistochemistry

Hypothesis: We hypothesize that predominately neurons and a few microglia will express Frz1 and this expression will decrease after stroke. **Rationale:** Wnt3a is known to bind to Frz1a, expressed by dendrites (Oderup *et al.*, 2013) and microglia, which may play a role in the regulation of apoptosis in neurons. Additionally, GSK3β is part of the

destruction complex (APC, Axin, and CK1) (Minde *et al.*, 2011) of β-catenin and can be regulated by these intrinsic proteins, a process in which PIWIL1a may be a significant player.

Aim1f: To Evaluate the Sexual Dimorphism in Male and Female Rats after MCAO and Treatment with Wnt3a

Hypothesis: We expect that wnt3a will help both sexes in preventing neuronal apoptosis and improve neurological results. **Rationale:** In the human population, the Framinham Heart Study reported that women had a lower risk of stroke compared to men, however in old age, women had a higher incidence of stroke and diminished functional outcome (Petrea et al., 2009). In rodent models, adult female rodents develop smaller infarct volumes and improved neurobehavioral outcomes following MCAO compared to their age-matched male rats; however, this effect was reversed in aged female rodents (Manwani et al., 2014). Therefore, we expect female rats to have an improved neurological benefit with wnt3a compared to their male counterpart. **Experimental Groups:** male sham, male+MCAO+Vehicle, male+MCAO+wnt3a, female sham, female+MCAO+Vehicle, female+MCAO+wnt3a.

Aim1g: To Determine the Age-related Differences in Young vs Old MCAO Rats Treated with Wnt3a

Hypothesis: We hypothesize that wnt3a will significantly improve behavioral and memory results following MCAO. **Rationale:** The incidence of stroke increases exponentially with age, with a 100-fold increase in rates between the 3rd and 4th decades

and the 8th and 9th decades (Bonita, 1992). Specifically, 92% of ischemic stroke occurs in people over the age of 65 and this needs to be simulated in the animal model. With aging, there is a strong association with a significant increase in cerebral infarct size and high mortality in stroke (Davis et al., 1995). Therefore, we will use middle (12 month) and old (18 month) aged male Sprague-dawley rats (Tan et al., 2013) to simulate the impact of age in stroke and drug efficacy.

Experimental groups: Middle-aged + male + Sham, middle-aged + male + MCAO + Vehicle, middle-aged + male + MCAO + wnt3a. old-aged + male + Sham, old-aged + male + MCAO + Vehicle, old-aged + male + MCAO + wnt3a.

Aim1h: To Evaluate Wnt3a Treatment in a Different Permanent Occlusion Model Compared to the Reperfusion Model of MCAO

Hypothesis: We hypothesize that the permanent occlusion might reduce the anti-apoptotic effects of wnt3a, but still should see improved neurological function compared to MCAO vehicle. **Rationale:** About half of the stroke patients in the United States result from large vessel occlusion (LVO, i.e. middle cerebral artery (M1 and M2 segments), internal carotid artery) (Rai, 2015) and only 15% are treated with tPA and about 4% are treated with mechanical embolectomy (González et al., 2013). Therefore, the transient model only represents 3-10% of all large vessel stroke patients (Kahle and Bix, 2012) and a pMCAO model would truly see the translational effectiveness of wnt3a as a therapy for patients that do not receive rTPA. Therefore, the permanent occlusion of the MCA will result in a decreased amount of wnt3a reaching the affected area, but, from

contralateral blood flow, we do expect some wnt3a to reach the penumbra and improve behavioral outcomes.

Experiment: For permanent occlusion, animals will undergo MCAO as previously described, but will not be re-perfused, the suture will be left tied off. The animal will be sutured and allowed to recover with the suture in place; behavioral results will be evaluated accordingly after recovery. **Experimental groups: 24 h endpoints:** Sham, permanent-MCAO+vehicle, permanent-MCAO+wnt3a.

Specific Aim Two

Determine the role of iN wnt3a in attenuation of apoptosis via regulation of the Frz1/PIWIL1a/FOXM1 pathway with subsequent down regulation of Caspase-3 and reduction of apoptotic neuronal cells after MCAO in rats. Our hypothesis is that Frz1, activated by iN wnt3a, will upregulate PIWI1a with downstream activation of FOXM1 and subsequently downregulate Caspase3 to reduce neuronal apoptosis after ischemic stroke. Therefore, the amelioration of neuronal cell death, post-ischemic stroke, will improve neurobehavioral outcomes. Two interventional approaches will be used to test this hypothesis: 1) siRNA inhibition of PIWIl1 and 2) a combination of siRNA inhibition of Frzld-1 and CRISPR activation of PIWIL1a. These hypotheses will be investigated in four sub-aims: A) Demonstrate that iN wnt3a induced reduction of neuronal cell death after ischemic stroke B) Determine the endogenous levels of wnt3a, Frz1, PIWIL1, GSK3β, β-catenin, FOXM1, and Caspase-3 before and after ischemic stroke C) Determine the effect of iN wnt3a on expression of Frz1, PIWI1a, GSK3-β, β-catenin,

FOXM1, and Caspase-3 after ischemic stroke D) Determine the effect of Frz1, PIWIL1 inhibition, and rescue in the wnt3a treated groups.

Aim2a: Evaluate Effect of iN Wnt3a on Apoptotic Neurons with Fluoro-Jade after Ischemic Stroke

Hypothesis: iN administration of wnt3a after ischemic stroke will reduce apoptotic pathways and up-regulate survival mechanisms. **Rationale:** The goal of this aim is to establish the role of iN wnt3a in reducing the number of apoptotic neurons. Previous studies have shown that wnt3a upregulates FOXM1, which then binds to β-catenin with subsequent migration to the nucleus (Zhang et al., 2011). Others studies have shown that FoxM1 has a direct impact on Caspase-3, but no mechanistic link has been established to this point between wnt3a and caspase-3 (Jiang et al., 2014). We expect these pathways to be upregulated and reduce the number of apoptotic cells.
Experiments: Animals will be sacrificed at 1 and 3 days after surgery, based on previous studies that have evaluated the development of apoptosis after ischemic stroke (Xu et al., 2006), and brain tissues will be collected for analysis via Fluoro–J to measure the presence of apoptotic neurons.
Experimental Groups: Sham, MCAO + Vehicle, MCAO + iN Wnt3a with immunohistochemistry at 24 h after surgery.

Aim 2b: Evaluate the Levels of Frz1, PIWIL1, GSK3-β, β-catenin, FOXM1, and Caspase-3 with Ischemic Stroke and after Treatment

Hypothesis: MCAO in rats will decrease wnt3a-dependent activation of the

Frz1→PIWIL1a→β-catenin pathway with resultant increase in expression of FoxM1. **Rationale:** Animal models of ischemic stroke have shown an increased neuronal apoptosis following ischemic injury and higher expression of caspase-3 in animal models. Western blots will quantify levels of wnt3a, Frz1, PIWI1, pGsk-3β, β-catenin, FOXM1, and CC-3 24 and 72 h after MCAO.

Experiments: Ischemic stroke was induced in animals using a MCAO model. Protein levels of proposed pathway in the brain samples will be measured via Western blot in sham and at 24 and 72 hours after MCAO. Antibodies for wnt3a, Frz1, PIWIL1a, pGSK3-β, β-catenin, FOXM1, and Caspase-3 will be used in our analysis.
Experimental Groups: Sham, MCAO+Saline, MCAO+wnt3a.

Aim 2c: Determine the Effect of PIWIL1a and Frz1 Inhibition to Establish Wnt3a's Mediated Anti-apoptotic Effect

Hypothesis: Wnt3a-induced activation of the Frz1 pathway will attenuate MCAO-induced caspase-3 upregulation and subsequent apoptosis; inhibition of this pathway will reduce the anti-apoptotic effects of wnt3a. **Rationale:** Wnt3a has been shown to increase FoxM1 in glioma cells (Zhang et al., 2011), and PIWIL1a, a protein that binds to piRNA, is known to up-regulate β-catenin, but a direct link between PIWIL1a and FoxM1 is yet to be investigated. To explore the postulated mechanism, we will utilize specific siRNAs of Frz1 and PIWI1a in combination with treatment.
Experiments: siRNAs of Frz1, and PIWI1a will be administered 1 hour prior to ischemic stroke induction and 5 hours after MCAO. iN wnt3a, dose and timing optimization in prior aim, will be administered post-MCAO. Animals will be sacrificed at 24 hours for

Western blot analysis to detect molecules involved in wnt3a anti-apoptotic signaling. Western blots will be performed to measure the expression of wnt3a, Frz1, PIWI1a, GSK3-β, β-catenin, FOXM1, and Caspase-3. Antibodies for wnt3a, Frz1, PIWI1, GSK3-β, β-catenin, FOXM1, and Caspase-3 will be used for our analysis.

Experimental Groups: Sham, MCAO+vehicle, MCAO+wnt3a, MCAO+Wnt3a+scrambled-siRNA MCAO+Wnt3a+PIWIL1a siRNA, MCAO+Wnt3a+Frz1a siRNA+PIWIL1a CRISPR control, MCAO+Wnt3a+Frz1a siRNA+PIWIL1a CRISPR activation.

Aim 2d: Determine the Effect of PIWIL1a Activation via CRISPR after Frz1 siRNA

Hypothesis: We hypothesize that although Frz1 is inhibited with an siRNA, the activation of PIWIL1a with CRISPR will up-regulate the survival protein FOXM1 and rescue the cell from apoptosis.

Experiments: siRNAs of Frz1, PIWI1a and PIWI1a CRISPR will be administered 24 hours prior to ischemic stroke induction. iN wnt3a, dose and timing optimized in prior aim, will be administered post-MCAO. Animals will be sacrificed at 24 hours for Western blot analysis to detect molecules involved in wnt3a anti-apoptotic signaling. Western blots will be performed to measure the expression of wnt3a, Frz1, PIWIL1, pGSK3-β, β-catenin, FOXM1, and CC-3.

Experimental Groups: Sham, MCAO+Vehicle, MCAO+Wnt3a, MCAO+Wnt3a+CRISPR control, MCAO+Wnt3a+Frz1a siRNA + PIWIL1a CRISPR, MCAO + Frz1a siRNA + PIWIL1a CRISPR.

Anticipated Results: We expect that iN administration of wnt3a will increase expression of PIWIL1a and FoxM1 in neurons. Their activity will down regulate levels of Gsk3-β, and Caspase-3, respectively, to reduce apoptosis in neuronal cells. Pharmacological inhibition of PIWIL1a will reduce the anti-apoptotic effect of wnt3a, but with the treatment of the CRISPER, PIWL1a should rescue the neuron via the proposed pathway, even after the inhibition of Frz1a.

The **long-term goal** of this proposal is to provide a basis for clinical translation of wnt3a as an effective therapeutic alternative to protect against complications secondary to cerebral ischemic stroke and to improve long-term patient outcomes.

References

Anon (1985) MRC trial of treatment of mild hypertension: principal results. Medical Research Council Working Party. Br Med J Clin Res Ed 291:97–104.

Arrázola MS, Silva-Alvarez C, Inestrosa NC (2015) How the Wnt signaling pathway protects from neurodegeneration: the mitochondrial scenario. Front Cell Neurosci 9 Available at: http://www.ncbi.nlm.nih.gov/pmc/articles/PMC4419851/ [Accessed July 13, 2015].

Ay H, Furie KL, Singhal A, Smith WS, Sorensen AG, Koroshetz WJ (2005) An evidence-based causative classification system for acute ischemic stroke. Ann Neurol 58:688–697.

Bonita R (1992) Epidemiology of stroke. The Lancet 339:342–344.

Broughton BRS, Reutens DC, Sobey CG (2009) Apoptotic Mechanisms After Cerebral Ischemia. Stroke 40:e331–e339.

Candelario-Jalil E (2009) Injury and repair mechanisms in ischemic stroke: considerations for the development of novel neurotherapeutics. Curr Opin Investig Drugs Lond Engl 2000 10:644–654.

Cerpa W, Toledo EM, Varela-Nallar L, Inestrosa NC (2009) The role of Wnt signaling in neuroprotection. Drug News Perspect 22:579–591.

Chacón MA, Varela-Nallar L, Inestrosa NC (2008) Frizzled-1 is involved in the neuroprotective effect of Wnt3a against Abeta oligomers. J Cell Physiol 217:215–227.

Davis M, Mendelow AD, Perry RH, Chambers IR, James OF (1995) Experimental stroke and neuroprotection in the aging rat brain. Stroke 26:1072–1078.

DeWood MA, Spores J, Notske R, Mouser LT, Burroughs R, Golden MS, Lang HT (1980) Prevalence of total coronary occlusion during the early hours of transmural myocardial infarction. N Engl J Med 303:897–902.

Ferrer I, Planas AM (2003) Signaling of cell death and cell survival following focal cerebral ischemia: life and death struggle in the penumbra. J Neuropathol Exp Neurol 62:329–339.

Ferri KF, Kroemer G (2001) Organelle-specific initiation of cell death pathways. Nat Cell Biol 3:E255-263.

González RG, Furie KL, Goldmacher GV, Smith WS, Kamalian S, Payabvash S, Harris GJ, Halpern EF, Koroshetz WJ, Camargo ECS, Dillon WP, Lev MH (2013) Good outcome rate of 35% in IV-tPA-treated patients with computed tomography

angiography confirmed severe anterior circulation occlusive stroke. Stroke 44:3109–3113.

Hankey GJ (1999) Smoking and risk of stroke. J Cardiovasc Risk 6:207–211.

Hendaoui I, Lavergne E, Lee H-S, Hong SH, Kim H-Z, Parent C, Heuzé-Vourc'h N, Clément B, Musso O (2012) Inhibition of Wnt/β-catenin signaling by a soluble collagen-derived frizzled domain interacting with Wnt3a and the receptors frizzled 1 and 8. PloS One 7:e30601.

Horn IR, van den Berg BM, Moestrup SK, Pannekoek H, van Zonneveld AJ (1998) Plasminogen activator inhibitor 1 contains a cryptic high affinity receptor binding site that is exposed upon complex formation with tissue-type plasminogen activator. Thromb Haemost 80:822–828.

Inestrosa NC, Varela-Nallar L (2014) Wnt signaling in the nervous system and in Alzheimer's disease. J Mol Cell Biol 6:64–74.

Jiang L, Wang P, Chen L, Chen H (2014) Down-regulation of FoxM1 by thiostrepton or small interfering RNA inhibits proliferation, transformation ability and angiogenesis, and induces apoptosis of nasopharyngeal carcinoma cells. Int J Clin Exp Pathol 7:5450–5460.

Jin R, Yang G, Li G (2010) Inflammatory mechanisms in ischemic stroke: role of inflammatory cells. J Leukoc Biol 87:779–789.

Kahle MP, Bix GJ (2012) Successfully Climbing the "STAIRs": Surmounting Failed Translation of Experimental Ischemic Stroke Treatments. Stroke Res Treat 2012 Available at: http://www.ncbi.nlm.nih.gov/pmc/articles/PMC3544313/.

Kurisu K, Yenari MA (2017) Therapeutic hypothermia for ischemic stroke; pathophysiology and future promise. Neuropharmacology Available at: http://www.sciencedirect.com/science/article/pii/S0028390817303921 [Accessed March 26, 2018].

Lai TW, Zhang S, Wang YT (2014) Excitotoxicity and stroke: Identifying novel targets for neuroprotection. Prog Neurobiol 115:157–188.

Le DA, Wu Y, Huang Z, Matsushita K, Plesnila N, Augustinack JC, Hyman BT, Yuan J, Kuida K, Flavell RA, Moskowitz MA (2002) Caspase activation and neuroprotection in caspase-3- deficient mice after in vivo cerebral ischemia and in vitro oxygen glucose deprivation. Proc Natl Acad Sci 99:15188–15193.

Leigh R et al. (2014) Pretreatment Blood–Brain Barrier Damage and Post-Treatment Intracranial Hemorrhage in Patients Receiving Intravenous Tissue-Type Plasminogen Activator. Stroke:STROKEAHA.114.005249.

Liu F, McCullough LD (2011) Middle Cerebral Artery Occlusion Model in Rodents: Methods and Potential Pitfalls. J Biomed Biotechnol 2011 Available at: https://www.ncbi.nlm.nih.gov/pmc/articles/PMC3035178/ [Accessed March 27, 2018].

López-Hernández FJ, Ortiz MA, Piedrafita FJ (2006) The extrinsic and intrinsic apoptotic pathways are differentially affected by temperature upstream of mitochondrial damage. Apoptosis 11:1339–1347.

Lott C, Hennes HJ, Dick W (1999) Stroke--a medical emergency. J Accid Emerg Med 16:2–7.

Mackay J, Mensah G (2004) Atlas of Heart Disease and Stroke, 1 edition. Geneva: World Health Organization.

Manwani B, Friedler B, Verma R, Venna VR, McCullough LD, Liu F (2014) Perfusion of ischemic brain in young and aged animals: a laser speckle flowmetry study. Stroke 45:571–578.

McCullough LD, Hurn PD (2003) Estrogen and ischemic neuroprotection: an integrated view. Trends Endocrinol Metab 14:228–235.

Minde DP, Anvarian Z, Rüdiger SG, Maurice MM (2011) Messing up disorder: how do missense mutations in the tumor suppressor protein APC lead to cancer? Mol Cancer 10:101.

Musuka TD, Wilton SB, Traboulsi M, Hill MD (2015) Diagnosis and management of acute ischemic stroke: speed is critical. CMAJ Can Med Assoc J 187:887–893.

Oderup C, LaJevic M, Butcher EC (2013) Canonical and non-canonical Wnt proteins program dendritic cell responses for tolerance. J Immunol Baltim Md 1950 190:6126–6134.

Peisker T, Koznar B, Stetkarova I, Widimsky P (2017) Acute stroke therapy: A review. Trends Cardiovasc Med 27:59–66.

Petrea RE, Beiser AS, Seshadri S, Kelly-Hayes M, Kase CS, Wolf PA (2009) Gender differences in stroke incidence and poststroke disability in the Framingham heart study. Stroke 40:1032–1037.

Rai AT (2015) Red pill, blue pill: reflections on the emerging large vessel stroke "market." J Neurointerventional Surg 7:623–625.

Reeves ME, Baldwin ML, Aragon R, Baldwin S, Chen S-T, Li X, Mohan S, Amaar YG (2012) RASSF1C modulates the expression of a stem cell renewal gene, PIWIL1. BMC Res Notes 5:239.

Roth JM (2011) Recombinant tissue plasminogen activator for the treatment of acute ischemic stroke. Proc Bayl Univ Med Cent 24:257–259.

Sacco RL, Benjamin EJ, Broderick JP, Dyken M, Easton JD, Feinberg WM, Goldstein LB, Gorelick PB, Howard G, Kittner SJ, Manolio TA, Whisnant JP, Wolf PA (1997) Risk Factors. Stroke 28:1507–1517.

Shabanzadeh AP, D'Onofrio PM, Monnier PP, Koeberle PD (2015) Targeting caspase-6 and caspase-8 to promote neuronal survival following ischemic stroke. Cell Death Dis 6:e1967.

Shruster A, Ben-Zur T, Melamed E, Offen D (2012) Wnt signaling enhances neurogenesis and improves neurological function after focal ischemic injury. PloS One 7:e40843.

Sun K, Fan J, Han J (2015) Ameliorating effects of traditional Chinese medicine preparation, Chinese materia medica and active compounds on ischemia/reperfusion-induced cerebral microcirculatory disturbances and neuron damage. Acta Pharm Sin B 5:8–24.

Tan Z, Turner RC, Leon RL, Li X, Hongpaisan J, Zheng W, Logsdon AF, Naser ZJ, Alkon DL, Rosen CL, Huber JD (2013) Bryostatin improves survival and reduces ischemic brain injury in aged rats after acute ischemic stroke. Stroke 44:3490–3497.

Xu X-H, Zhang S-M, Yan W-M, Li X-R, Zhang H-Y, Zheng X-X (2006) Development of cerebral infarction, apoptotic cell death and expression of X-chromosome-linked inhibitor of apoptosis protein following focal cerebral ischemia in rats. Life Sci 78:704–712.

Zhang N, Wei P, Gong A, Chiu W-T, Lee H-T, Colman H, Huang H, Xue J, Liu M, Wang Y, Sawaya R, Xie K, Yung WKA, Medema RH, He X, Huang S (2011) FoxM1 promotes β-catenin nuclear localization and controls Wnt target-gene expression and glioma tumorigenesis. Cancer Cell 20:427–442.

CHAPTER TWO

INTRANASAL WNT3A ATTENUATES NEURONAL APOPTOSIS THROUGH FRZ1/PIWIL1A/FOXM1 PATHWAY IN MCAO RATS

Nathanael Matei,[1] Justin Camara,[1] Devin M[c]Bride,[1,4] Richard Camara,[1] Ningbo Xu,[1] Jiping Tang,[1] John H. Zhang[1,2,3]

Departments of [1]Physiology and Pharmacology, [2]Anesthesiology and [3]Neurosurgery, Loma Linda University, Loma Linda, California 92354,

[4]The Vivian L. Smith Department of Neurosurgery, McGovern Medical School, The University of Texas Health Science Center at Houston, Houston, Texas 77030

Note: Most of this chapter is taken from a paper currently in the submission process

Abstract

Currently the only treatment available for stroke is tissue plasminogen activator and remains the only FDA approved pharmacological intervention. Therefore, the focus of our proposal is to use the potential neuroprotective agent wnt3a to protect against neurovascular unit damage in ischemic stroke by attenuating neuron apoptotic pathways. Wnt3a is a glycolipoprotein that is involved in many cellular functions, ranging from apoptosis, neurogenesis, embryonic development, adult homeostasis, and cell polarity. Recently, wnt3a has been descriptively shown to play a role in focal ischemic injury in the murine model. Several studies have shown wnt3a to be promising, up-regulating FoxM1, a survival protein.

The focus of our proposal is to use wnt3a to attenuate apoptosis in neurons. Our overall hypothesis is that wnt3a will provide therapeutic benefits following ischemic stroke in rats via the reduction of Gsk3β and Caspase-3 to promote neuronal survival. Our hypothesis is that Frz1, activated by wnt3a, will upregulate PIWIL1a with down-stream activation of Foxm1, which will reduce Caspase-3, lowering the overall neuronal apoptosis after stroke.

Abbreviations

LD	Low Dose (0.4 µg/kg)
HD	High Dose (1.2 µg/kg)
FRZ1	Frizzled-1
MCAO	Middle Cerebral Artery Occlusion
rtPA	Recombinant Tissue Plasminogen Activator
BBB	Blood Brain Barrier
CNS	Central Nervous System
LRP5/6	Lipoprotein receptor related proteins 5 and 6
CC-3	Cleaved Caspase-3
CRISPR	Clustered Regularly Interspaced Short Palindromic Repeats

Introduction

Stroke is an acute onset disturbance of cerebral function due to ischemia or hemorrhage. Ischemic stroke is the 3rd leading cause of mortality globally and the number one cause of disability (Mackay & Mensah, 2004). Two approaches have been pursued to reduce the disease burden of stroke—neuroprotection and reperfusion (Fisher & Brott, 2003). Of these two, only reperfusion has had success in human clinical trials in the form of pharmacological recombinant tissue plasminogen activator (rtPA) intervention and mechanical clot disruption (Rha & Saver, 2007). rtPA continues to be the only FDA approved pharmacological intervention approved for acute ischemic stroke despite multiple clinical trials exploring alternative treatments (Roth, 2011). Thus, we evaluated the potential neuroprotective agent wnt3a to protect against neuronal damage caused by ischemic stroke.

Wnt3a is a glycolipoprotein that controls important cellular functions including apoptosis, neurogenesis, embryonic development, adult homeostasis, and cell polarity (MacDonald *et al.*, 2009; Zhang *et al.*, 2011; Wu *et al.*, 2014). Nineteen different isoforms of "wnt" all bind to the N-terminal extra-cellular cysteine-rich domain of Frizzled (Frz) family receptor, a serpentine G-protein receptor (Rao & Kühl, 2010), which has its own specific isoforms. Each wnt isoform has specific innate functions dependent in part on cell type. For example, in dendritic cells the wnt3a isoform upregulates VEGF, whereas the wnt5a isoform induces IL-10 through alternative pathways (Oderup *et al.*, 2013). Although the wnt pathway has been studied extensively, the identification of new isoforms of wnt and their unique mechanistic endpoints have

revived therapeutic interest in wnt (Cerpa *et al.*, 2009; Shruster *et al.*, 2012; Inestrosa & Varela-Nallar, 2014).

Recent studies have targeted GSK-3β reduction to improve outcomes after ischemic stroke. In the diabetic ischemic stroke rat model, insulin, an inhibitor of the activation of GSK-3β (Cohen & Goedert, 2004), and TDZD-8, a selective inhibitor of GSK-3β, both reduced the severity of the deleterious consequences of stroke-- reducing the infarct volume and lowering the expression of GSK-3β (Collino *et al.*, 2009). Convincingly establishing a role for GSK3β in stroke pathology, Kelly et al. showed that inhibition of GSK3β with CXhir025 in both OGD *in vitro* and *in vivo* rat MCAO models increased neuronal cell survival (Kelly *et al.*, 2004). In the intracerebral hemorrhage mouse model, 6-bromoindirubin-3′-oxime, a selective GSK-3β inhibitor, acutely administered, reduced hematoma volume by attenuating the expression of GSK-3β phosphorylation/activation, which increased the viability of neurons and other cell types (Zhao *et al.*, 2017). These findings suggest that the wnt/GSK-3β/β-catenin pathway may be further explored for treatment in the pathology of stroke.

In this study, the novel glycolipoprotein wnt3a is used for the very first time as an intranasal therapy to influence the pathophysiology of stroke in the MCAO model. Other studies of wnt3a have found that it prevents apoptosis (Reeves *et al.*, 2012) and is neuroprotective, but the mechanistic understanding is limited. Researchers showed that PIWL1a (Reeves *et al.*, 2012) directly affects the regulation of β-catenin in a cell-survival pathway in lung cancer cells, but further research is needed to establish the relationship between PIWIL1a and wnt3a in stroke. Reports have linked β-catenin with FOXM1 (Zhang *et al.*, 2011), and both have been linked to the inhibition of apoptosis (Jiang *et al.*,

2014).

To date, there are 10 human G protein-coupled Frizzled receptors, but only Frz1 has been supported in literature to be activated by the binding of wnt3a (Chacón *et al.*, 2008; Oderup *et al.*, 2013; Wu *et al.*, 2014; Arrázola *et al.*, 2015; "Wnt Receptors & Pathways: R&D Systems," 2018). Although wnt3a is known to bind to Frz1, the intracellular pathway triggered within neurons remains poorly investigated. In the present study, we hypothesize the effect of intranasal wnt3a on its downstream targets, Frizzled1/PIWI1a/FOXM1, will attenuate neuronal apoptosis in the rat model of transient MCAO. (Fig. 1).

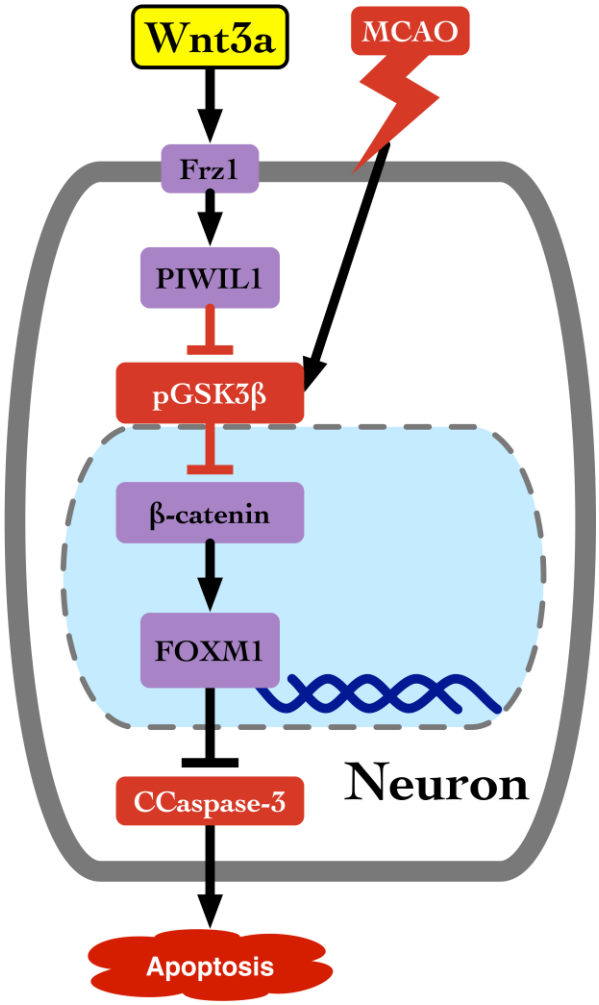

Figure 1. Proposed pathway for wnt3a activation of Frizzled1 and its downstream targets. Wnt3a binds to Frizzled-1, increases PIWIL1a, inhibits the activation of GSK3β, and activates β-catenin, which translocates into the nucleus to increase the transcription of FOXM1—a survival protein that inhibits apoptosis.

Materials and Methods

Animals

All experiments were approved by the Institutional Animal Care and Use Committee of Loma Linda University, complied with the National Institutes of Health's Guide for the Care and Use of Laboratory Animals, and are reported according to the ARRIVE (Animal Research: Reporting of In Vivo Experiments) guidelines. Animals were housed in a 12 h light-dark cycle, temperature-controlled room. Animals were divided into groups in a randomized fashion and experiments were performed in a blinded manner.

Laboratory Animals

Adult male (weighing 250-300g), aged male (weighing 400g at 9 months old), female (weighing 240-250g) Sprague Dawley rats were used in the proposed study.

Experimental Design

A total of 229 rats were used. Experiment 1 characterized the endogenous time-course of wnt3a, Frz1, PIWI1a, p-GSK3β, FOXM1, and CC-3 in the right hemisphere at 6, 12, 24, and 72 h after MCAO. Twenty-six rats were used in the following groups: sham (n=4), 6 (n=5), 12 (n=6), 24 (n=6), and 72 h (n=5).

Experiment 2 evaluated the role of wnt3a in the pathophysiology of MCAO as follows. First, we tested the effect of iN wnt3a. 203 rats were used in the following groups: 24 hour endpoints: sham (n=11), MCAO + vehicle (n=14), MCAO + wnt3a LD (0.4 µg/kg) (n=8), MCAO + wnt3a HD (1.2 µg/kg) (n=13), MCAO + wnt3a + scrambled

siRNA (n=7), MCAO + wnta3a + Frz1-siRNA (n=8), MCAO + wnt3a + PIWI-siRNA (n=8), MCAO + wnt3a + scrambled CRISPR (n= 7), MCAO + wnt3a + PIWI CRISPR + Frz1-siRNA (n= 7); female: sham (n=6), MCAO + vehicle (n=8), MCAO + wnt3a HD (1.2 µg/kg) (n=8); aged-rats: sham (n=6), MCAO + vehicle (n=7), MCAO + wnt3a HD (1.2 µg/kg) (n=6); pMCAO: MCAO + vehicle (n=10), MCAO + wnt3a HD (1.2 µg/kg) (n=9); Naïve groups: Naïve (n=6), Naïve + scrambled siRNA (n=12), Naïve + Frz1-siRNA (n=6), Naïve + PIWI-siRNA (n=6), Naïve + PIWI1a CRISPR + Frz-1siRNA (n= 6). 72 h endpoints: Sham (n=6), MCAO + vehicle (n=8), MCAO + wnt3a HD (n=8). Recombinant mouse wnt3a (abcam; ab81484), used for all molecular and behavioral studies, and human GST tagged wnt3a (abcam; 153563), only used in Fig. 13 to confirm presence and delivery, were reconstituted in ddH_2O to yield 0.1 mg/ml and given at 0.4 µg/kg for the low dose or 1.2 µg/kg for the high dose. Five-hundred pmol of Frz1 (sc-39977 and AM16708) and PIWI1a (sc-40677 and AM16708) were dissolved in 2 µl of sterilized water and injected intracerebroventricularly 24 h before MCAO. The same volume of scramble siRNA (sc-37007 and AM4611) was administered as control. For PIWI1a-CRISPR activation, 2 ug in 2 ul (transfection medium and transfection reagent, described in the intracerebroventricular injection section) per animal was injected 24 h before MCAO (detailed in the Intracerebroventricular injection section). The control of a scrambled CRISPR was used with the same volume.

MCAO Model

Rats were anesthetized intraperitoneally with a mixture of ketamine (80 mg/kg) and xylazine (20 mg/kg), until no pinch-paw reflex was observed, and maintained

throughout the experiments. Body temperature and respiration rate were monitored perioperatively. A vertical midline cervical incision was made, and the right common carotid artery was exposed and dissected. All branches of the external carotid artery were isolated, coagulated, and transected, and then the external carotid artery was divided (leaving 3-4 mm). The internal carotid artery was isolated and the pterygopalatine artery was ligated close to its origin. A 5 mm aneurysm clip was used to clamp the common carotid artery. The external carotid artery stump was reopened and a 4.0 monofilament nylon suture with an enlarged, round tip was inserted through the internal carotid artery; insertion was stopped when resistance was felt, occluding the origin of the right MCA. After 2 hours of occlusion, the suture was withdrawn to allow for reperfusion. The external carotid artery was ligated, and the aneurysm clip was removed. The skin was sutured (1% lidocaine was applied) and the animal was allowed to recover. Sham surgery included the exposure of the common, external, and internal carotid arteries with all ligations and transections; no occlusion occurred in the sham group (Kusaka *et al.*, 2004; Chen *et al.*, 2011).

Intracerebroventricular Injection

As described previously (Liu *et al.*, 2007; Chen *et al.*, 2013), rats were anesthetized with isoflurane (4% induction, 2.5% maintenance) and mounted on a stereotaxic frame. The needle of a 10 μl Hamilton syringe was inserted through a burr hole perforated through the skull into the left lateral ventricle using the following coordinates relative to bregma: 1.5 mm posterior, 1.0 mm lateral, and 3.2 mm below the horizontal plane of the bregma. siRNA was injected 24 h before MCAO. According to

the manufacturer's instructions, a total volume of 2 ul (500 pmol) of siRNA in sterile saline was injected in ipsilateral ventricle at a rate of 0.5 ul/min. A combination of two siRNAs were used for Frz1 (sc-39977 and AM16708) and PIWI1a (sc-40677 and AM16708) providing advantages in both potency and specificity of gene silencing. The same volume of scramble siRNA (sc-37007 and AM4611) was used as a negative control. siRNA is a tool that induces short-term silencing of protein coding genes and targets a specific mRNA for degradation. To reverse the effects of siRNA, we will utilize an engineered form of clustered, regularly interspaced, short palindromic repeats (CRISPR) associated (Cas) protein system (Jinek *et al.*, 2012). Briefly, in this system, the type II CRISPR protein Cas9 is directed to genomic target sites by short RNAs, where it functions as a endonuclease, which can inactivate or activate genes (Perez-Pinera *et al.*, 2013)—used successfully in plants and animals, both vertebrae and invertebrae (Horvath & Barrangou, 2010; Gratz *et al.*, 2013; Jiang *et al.*, 2013; Mali *et al.*, 2013; Bortesi & Fischer, 2015). CRISPR will be used to activate PIWI1a expression in the rat brain. A total of 4 ul of active PIWI1a CRISPR (sc-418611) was injected 24 h before MCAO. 20 ug of CRISPR was suspended in 20ul of plasmid transfection medium (sc-108062) and activated with another 20 ul of transfection reagent (sc-395739), totaling 2ug per animal of active CRISPR. The control scrambled CRISPR (sc-437275) followed the same steps and a total of 2ug per animal was given ICV. To prevent possible leakage, the needle was kept *in situ* for an additional 10 min after completing the injection and then withdrawn slowly over 5 min. After removal of the needle, the burr hole was sealed with bone wax, the incision was sutured, and the rats were allowed to recover.

2, 3, 5-Triphenyltetraolium Chloride Staining

As described previously (Hu *et al.*, 2009), 2,3,5-triphenyltetrazolium chloride monohydrate staining was performed to determine the infarct volume at 24hr and 72hr after MCAO. The possible interference of brain edema with infarct volume was corrected (whole contralateral hemisphere volume minus non-ischemic ipsilateral hemisphere volume) and the infarcted volume was expressed as a percentage of the whole contralateral hemisphere (McBride *et al.*, 2016).

Immunofluorescence Staining

Immunohistochemistry was performed as described previously (Chen *et al.*, 2013). Briefly, rats were perfused with cold PBS under deep anesthesia, followed by infusion of 4% formalin 24h after MCAO. The brains were harvested and immersed in 4% formalin at 4°C, then dehydrated with 30% sucrose for seven days, then mounted in OCT and frozen. After cryosectioning into 10μm thick sections, slices were incubated with the primary antibodies goat anti-Frz1 (1:100) (PA5-47072), rabbit anti-NeuN (1:200)(ab177487), rabbit anti-GFAP (1:100)(ab16997), goat anti-ionized calcium binding adaptor molecule 1 (IBA1, 1:200; Abcam), followed by incubation with appropriate secondary antibodies conjugated with either FITC (Neun, GFAP, Iba1) or Rodamine Red (Frz1) (Jackson ImmunoResearch). Negative control staining was performed by omitting the primary antibody. The sections were visualized with a fluorescence microscope (Lieca).

Western Blots

Western blotting was performed as described previously (Ayer *et al.*, 2012; Chen *et al.*, 2013). At each time point, rats were perfused with cold PBS, pH 7.4, solution delivered via intracardiac injection, followed by dissection of the brain into right frontal, left frontal, right parietal, left parietal, cerebellum, and brainstem. The brain parts were snap frozen in liquid nitrogen and stored at −80°C for subsequent analysis. Right hemisphere protein extraction from whole-cell lysates were obtained by gently homogenizing the hemisphere in RIPA lysis buffer (Santa Cruz Biotechnology) with further centrifugation at 14,000 × *g* at 4°C for 30 min. The supernatant was used as whole-cell protein extract, and the protein concentration was determined using a detergent-compatible assay (Bio-Rad). Equal amounts of protein were loaded on an SDS-PAGE gel. After being electrophoresed and transferred to a nitrocellulose membrane, the membrane was blocked and incubated with the primary antibody overnight at 4°C. The primary antibodies were rabbit polyclonal anti-wnt3a (1:1000; ab28472), rabbit polyclonal anti-Frz1 (1:1000; ab126262), rabbit polyclonal anti-PIWI1a (1:1000; ab12337), mouse monoclonal anti-β-catenin (1:1000; ab32572), rabbit polyclonal anti-pGsk-3β (1:1000; ab75745), rabbit polyclonal anti-FOXM1 (1:1000; sc-376471), rabbit polyclonal anti-CC3 (1:1000; ab13847), rabbit polyclonal anti-GST (ab 19256), rabbit monoclonal anti-LRP6 (1:1000; ab134146), and rabbit polyclonal anti-phospho-LRP6 (1:500; 2568s). For loading control, the same membranes were blotted with primary antibody of goat anti-β-actin (1:1000; sc-1616). Nitrocellulose membranes were incubated with appropriate secondary antibodies (1:2000; Santa Cruz Biotechnology) for 30 min at room temperature. Immunoblot bands were further probed with a

chemiluminescence reagent kit (ECL Plus; GE Healthcare). Data was analyzed by blinded researchers using ImageJ software, and each protein was normalized to their respective β-actin bands.

Neurobehavioral Testing

Neurobehavioral outcomes were assessed by a blinded observer at 24 and 72 h post-MCAO using the Modified Garcia Score (Kusaka *et al.*, 2004; Chen *et al.*, 2010). Animal scores for sensorimotor functions evaluated six parameters: spontaneous activity, symmetry in the movement of all four limbs, forepaw outstretching, climbing, body proprioception, and response to vibrissae touch. A maximum score of 21 was given with higher scores indicating better performance.

Left-forelimb Testing

Vibrissae evoked forelimb placing test was assessed by a blinded observer at 24 h and 72 h post-MCAO. Left fore-limb testing assesses for asymmetry in the sensorimotor cortex and striatum. The experimenter holds the animal so that all four limbs hang freely and the vibrissae are stimulated by sweeping each side against the edge of a table. This elicits an ipsilateral forelimb response to place the paw on the table top. The rat is stimulated 10 times on each side, and the total number of paw placements is recorded. *Water Maze.* Activity was evaluated for long term memory and learning. Briefly, the rat was placed in a pool (110 cm diameter) filled with water up to 15 cm from the upper edge. A platform (11cm diameter) was then submerged into the pool. An overhead camera was used to record the swim path, allowing for quantification of swim distance,

swim speed and time spent in the probe quadrant by a computerized tracking system (Noldus Ethovision; WA). The rats were first be trained using a cued water maze test. This test was used as a control to assess any sensorimotor and/or motivational deficits. In the cued test, the platform was made visible 5 mm above the water surface. The rat was released into the water and allowed to find the platform. Next, the spatial water maze test was performed in 5 blocks. In this test, the platform was submerged 1 cm below the surface of water. The location of the platform was changed for each block. Lastly, the rat was released into the water opposite the platform, and allowed to swim in the water to find the platform.

Fluoro-Jade C Staining

FJC staining was performed to detect degenerating neurons with a modified FJC ready-to-dilute staining kit (Biosensis, USA) according to the manufacturer's instructions (Schmued *et al.*, 2005). FJC-positive neurons in a 0.56mm^2 region of the ischemic boundary zone next to the ischemic core were counted in four randomly selected microscopic fields by an independent observer. Quantified analysis was performed by blinded researchers using Image J software. The data was presented as the number of FJC-positive neurons in the field of view.

Statistical Analysis

Quantitative data are presented as mean ± SD. One-way ANOVA with *post-hoc Tukey* test was used to determine significant group differences among groups at each time point for infarction volume and Western blot data. For non-parametric data, One-way

ANOVA-Wallis with Dunn's post-hoc was used to analyze neurobehavioral data after deviation from normality was confirmed. $p < 0.05$ was considered statistically significant. GraphPad Prism 6 (La Jolla, CA, USA) was used for graphing and analyzing all data.

Results

All sham-operated rats survived, but the overall mortality of MCAO was 21.94%. The mortality was not significantly different among the experimental groups (data not shown).

Endogenous Expressions of wnt3a and FRZ1/PIWI1/FOXM1 were Decreased in Neurons 24 hours after MCAO, While the Proteins Caspase 3 and GSK3-β were Increased

Western blot was used to detect time-course expression of wnt3a, Frzd1, PIWI1a, FOXM1, pGSK-3β, and CC-3 in brain tissue at baseline, 6, 12, 24, and 72 h after MCAO (Figure 2). Representatives immunoblots are shown in Fig. 2A. The expression pattern of wnt3a (Fig. 2B) and Frz1 (Fig. 2C) showed a significant decrease from 6 to 72 h after MCAO (Fig. 2B). PIWI1a was significantly decreased from 12 to 24 h after MCAO, but indistinguishable at 72 h compared to sham (Fig. 2D). After MCAO, p-GSK3β increased significantly from 12 to 72 h compared to sham (Fig. 2E). Survival protein FOXM1 was significantly decreased from 6 to 72 h after MCAO (Fig. 2F). In contrast, apoptotic protein CC-3 was significantly increased from 6 h to 72 h after MCAO (Fig. 2G). Extended Fig. 2-1 reports the specific statistics for each group comparison.

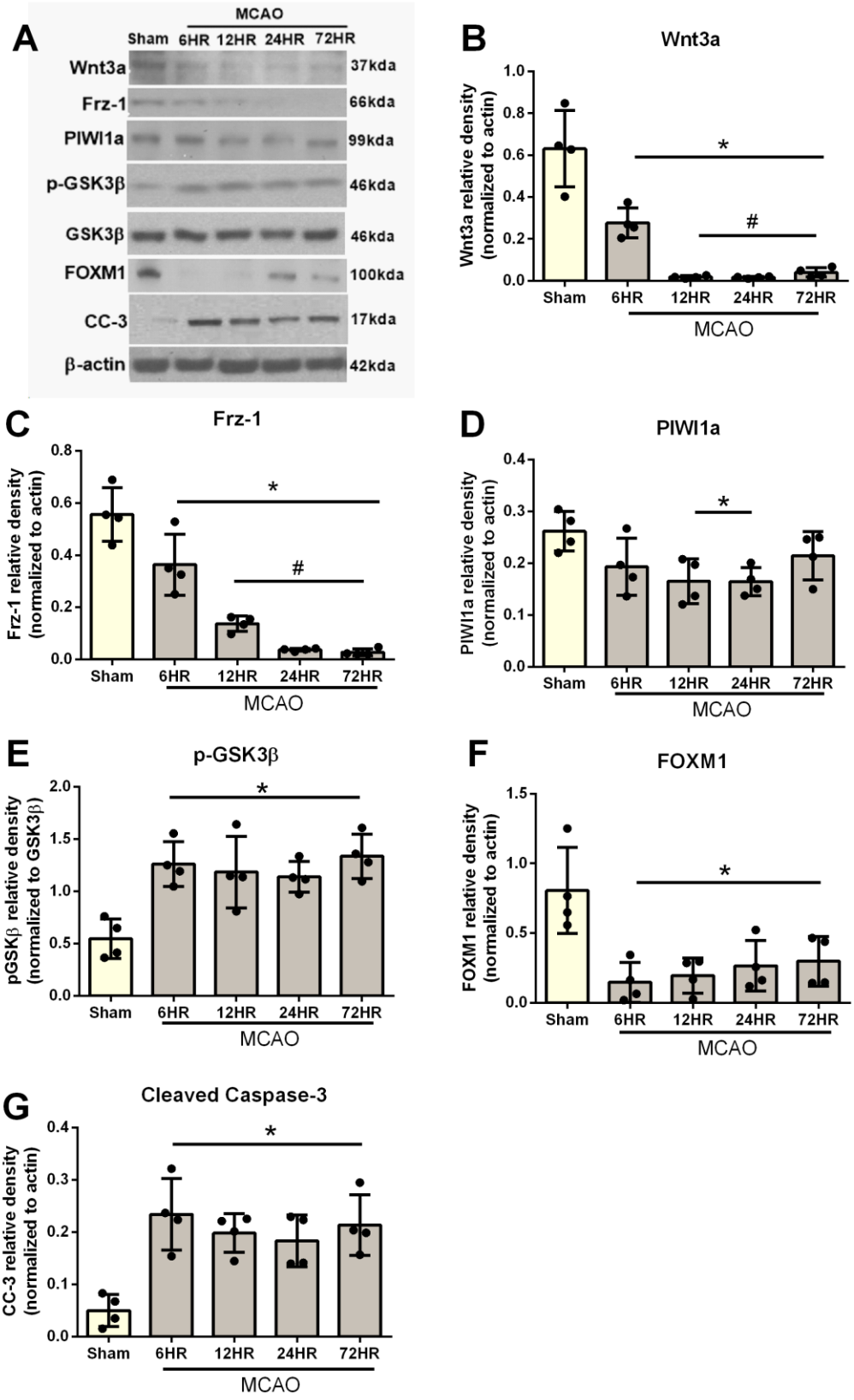
A
MCAO
Sham 6HR 12HR 24HR 72HR
Wnt3a 37kda
Frz-1 66kda
PIWI1a 99kda
p-GSK3β 46kda
GSK3β 46kda
FOXM1 100kda
CC-3 17kda
β-actin 42kda
B
Wnt3a
Wnt3a relative density (normalized to actin)
Sham 6HR 12HR 24HR 72HR
MCAO
C
Frz-1
Frz-1 relative density (normalized to actin)
D
PIWI1a
PIWI1a relative density (normalized to actin)
E
p-GSK3β
pGSKβ relative density (normalized to GSK3β)
F
FOXM1
FOXM1 relative density (normalized to actin)
G
Cleaved Caspase-3
CC-3 relative density (normalized to actin)

Figure 2. Time course of wnt3a, Frz1, PIWI1a, pGsk-3β, FOXM1, and CC3 in the right hemisphere of the rat brain after MCAO. (A) Representative Western blots. Quantitative analysis with western blot showed that the expression of (B) Wnt3a and (C) Frz1 significantly decreased by 6 hours. (D) PIWI1a was decreased by 12 hours and returned to sham levels by 72 hours. (E) However, pGsk-3β was increased after MCAO. (F) FOXM1 was decreased after MCAO, but (G) CC3 was increased. Each column represents the mean ± SD (n=4/group). *$p<0.05$ vs. Sham, #$p<0.05$ vs 6Hr. Extended Fig. 2-1 reports the specific statistics for each group comparison.

Time-course					
Protein	Tukey's multiple comparisons test	Mean Diff.	95% CI of diff.	DF	p-value
wnt3a	Sham vs. 6HR	0.3546	0.1622 to 0.5469	15	0.0004
	Sham vs. 12HR	0.6127	0.4203 to 0.8050	15	< 0.0001
	Sham vs. 24HR	0.6143	0.4219 to 0.8067	15	< 0.0001
	Sham vs. 72HR	0.5908	0.3984 to 0.7832	15	< 0.0001
	6HR vs. 12HR	0.2581	0.06571 to 0.4505	15	0.0066
	6HR vs. 24HR	0.2597	0.06736 to 0.4521	15	0.0063
	6HR vs. 72HR	0.2362	0.04383 to 0.4286	15	0.013
	12HR vs. 24HR	0.00165	-0.1907 to 0.1940	15	> 0.9999
	12HR vs. 72HR	-0.02188	-0.2143 to 0.1705	15	0.9964
	24HR vs. 72HR	-0.02353	-0.2159 to 0.1688	15	0.9952
Frz1	Sham vs. 6HR	0.193	0.03732 to 0.3486	15	0.0121
	Sham vs. 12HR	0.4194	0.2638 to 0.5751	15	< 0.0001
	Sham vs. 24HR	0.5192	0.3636 to 0.6748	15	< 0.0001
	Sham vs. 72HR	0.5286	0.3730 to 0.6843	15	< 0.0001
	6HR vs. 12HR	0.2265	0.07085 to 0.3821	15	0.0033
	6HR vs. 24HR	0.3262	0.1706 to 0.4819	15	< 0.0001
	6HR vs. 72HR	0.3357	0.1800 to 0.4913	15	< 0.0001
	12HR vs. 24HR	0.09976	-0.05588 to 0.2554	15	0.3214
	12HR vs. 72HR	0.1092	-0.04644 to 0.2648	15	0.2443
	24HR vs. 72HR	0.009434	-0.1462 to 0.1651	15	0.9997
PIWI1a	Sham vs. 6HR	0.06866	-0.02531 to 0.1626	15	0.2126
	Sham vs. 12HR	0.09636	0.002390 to 0.1903	15	0.0432
	Sham vs. 24HR	0.09746	0.003488 to 0.1914	15	0.0403
	Sham vs. 72HR	0.04744	-0.04653 to 0.1414	15	0.5431
	6HR vs. 12HR	0.0277	-0.06627 to 0.1217	15	0.8885
	6HR vs. 24HR	0.0288	-0.06517 to 0.1228	15	0.8742
	6HR vs. 72HR	-0.02121	-0.1152 to 0.07275	15	0.954
	12HR vs. 24HR	0.001097	-0.09287 to 0.09507	15	> 0.9999
	12HR vs. 72HR	-0.04892	-0.1429 to 0.04505	15	0.5151
	24HR vs. 72HR	-0.05001	-0.1440 to 0.04396	15	0.4944
p-GSK3β/GSK3β	Sham vs. 6HR	-0.1545	-0.3505 to 0.04153	15	0.0042
	Sham vs. 12HR	-0.2104	-0.4064 to -0.01444	15	0.0106
	Sham vs. 24HR	-0.2393	-0.4353 to -0.04330	15	0.0178
	Sham vs. 72HR	-0.3011	-0.4971 to -0.1051	15	0.0018
	6HR vs. 12HR	-0.05597	-0.2520 to 0.1400	15	0.9885
	6HR vs. 24HR	-0.08483	-0.2808 to 0.1112	15	0.9418
	6HR vs. 72HR	-0.1466	-0.3426 to 0.04937	15	0.9902
	12HR vs. 24HR	-0.02887	-0.2249 to 0.1671	15	0.9987
	12HR vs. 72HR	-0.09066	-0.2867 to 0.1053	15	0.8806
	24HR vs. 72HR	-0.06179	-0.2578 to 0.1342	15	0.7507
CC-3	Sham vs. 6HR	-0.1838	-0.2946 to -0.07304	15	0.001
	Sham vs. 12HR	-0.148	-0.2587 to -0.03721	15	0.0068
	Sham vs. 24HR	-0.1333	-0.2441 to -0.02255	15	0.0151
	Sham vs. 72HR	-0.1632	-0.2740 to -0.05243	15	0.003
	6HR vs. 12HR	0.03583	-0.07493 to 0.1466	15	0.8518
	6HR vs. 24HR	0.0505	-0.06027 to 0.1613	15	0.6323
	6HR vs. 72HR	0.02061	-0.09015 to 0.1314	15	0.9768
	12HR vs. 24HR	0.01467	-0.09610 to 0.1254	15	0.9935
	12HR vs. 72HR	-0.01522	-0.1260 to 0.09555	15	0.9925
	24HR vs. 72HR	-0.02989	-0.1407 to 0.08088	15	0.9161

Table 2-1. P values from each comparison in time-course study (Figure 2). One-way ANOVA with Tukey's multiple comparisons tests were run on western blot groups and the mean differences shown (n=4/group). *p<.05, **p<0.01, ***p<0.001, ****p<0.0001.

Effects of wnt3a on Infarction Size and Neurobehavioral Function 24 h after MCAO

Qualitative images of infarction volume in various groups are shown in Fig 3A, and quantitively, there was a significant reduction in infarction volume with high dosage (1.3 ug/kg) compared to vehicle (One-way ANOVA; Tukey's test; n=6-9; $F(3, 20) = 23.44$; $p=0.0153$) (Fig 3B). Wnt3a restored modified Garcia (Fig 3C) scores to sham levels and caused significant improvement in left-forelimb placement (Fig 3D) compared to vehicle (One-way ANOVA; Kruskal-Wallis with Dunn's post-hoc; n=6-9; $p=0.0031$) at 24 h. With the loss of oxygen and glucose, a hypoxic state is created in the acute stage of cerebral infarction, and recanalization triggers an apoptotic neuronal stress response (Candelario-Jalil, 2009)**.** Neuron survival is a key contributor to outcomes after stroke (Lai *et al.*, 2014). Thus, neuron protection is an important therapeutic target for the treatment of stroke (Cerpa *et al.*, 2009; Lai *et al.*, 2014). To evaluate the effects of intranasal (iN) wnt3a on neurological outcomes in transient focal cerebral ischemia, infarction volume and neurobehavior were assessed.

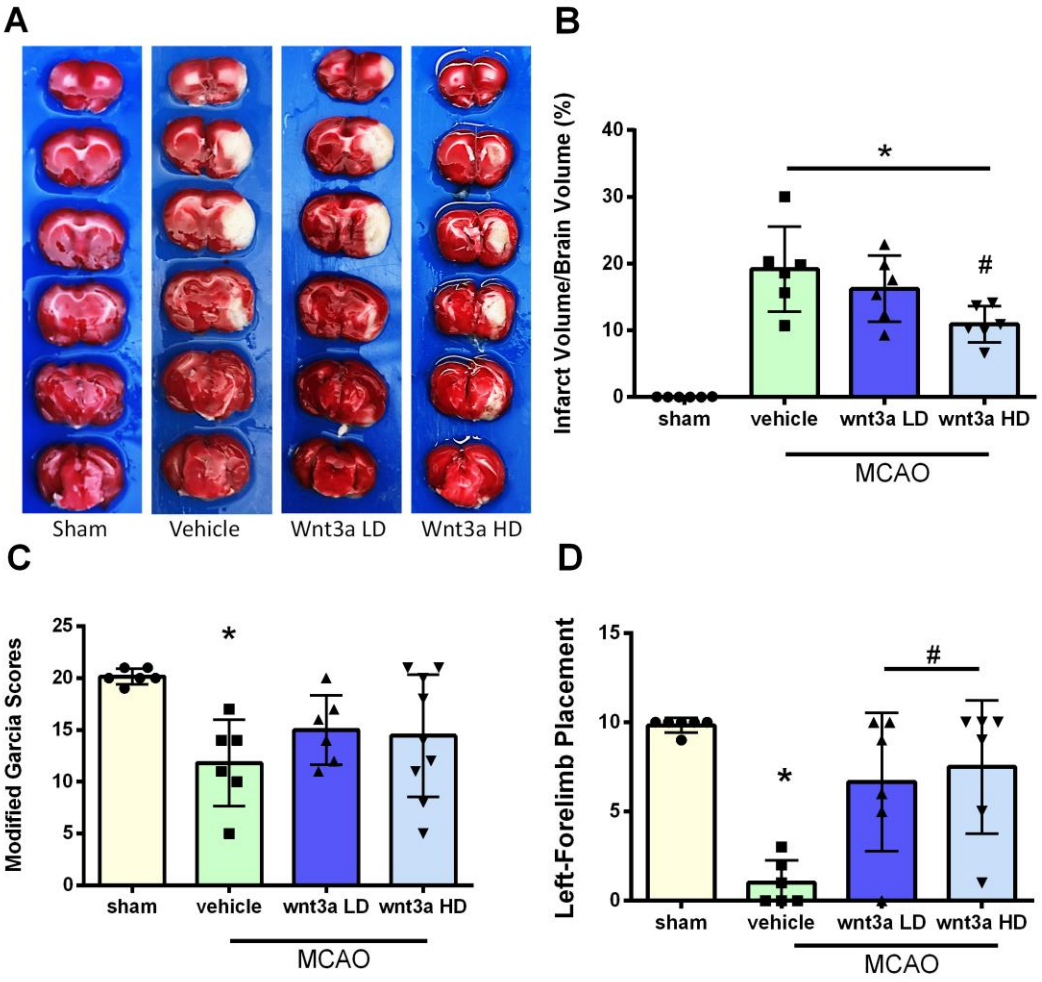

Figure 3. Wnt3a attenuated infarct volume and improved neurological function 24 hours after MCAO. (A) Representative TTC staining images of coronal sections. (B) Wnt3a HD (1.2 µg/kg) effectively reduced the infarct volume. (C) Modified Garcia Scores showed that low and high dose of wnt3a decreased neurological deficits. (D) Left-forelimb placement was improved in both the low and high doses of wnt3a. Each column represents the mean ± SD (n=6-9/group). *p<0.05 vs. Sham, #p<0.05 vs vehicle.

Wnt3a Reduced Apoptotic Cells after MCAO

Brain coronal sections obtained 24 h after MCAO were stained with Fluro-Jade-C (FJC) to present the number of degenerating cells in the penumbra of the cortex after ischemia/reperfusion (Fig 4A). Higher levels of FJC staining were observed in the MCAO group compared to the Sham group. Wnt3a significantly decreased the FJC positive cells in the penumbra compared to vehicle (67.00±14.24/field vs 193±30.84/field, One-way ANOVA; Tukey's test; $F(2,6) = 72.44$; $n=3$; $p<0.05$, for each) (Fig 4B).

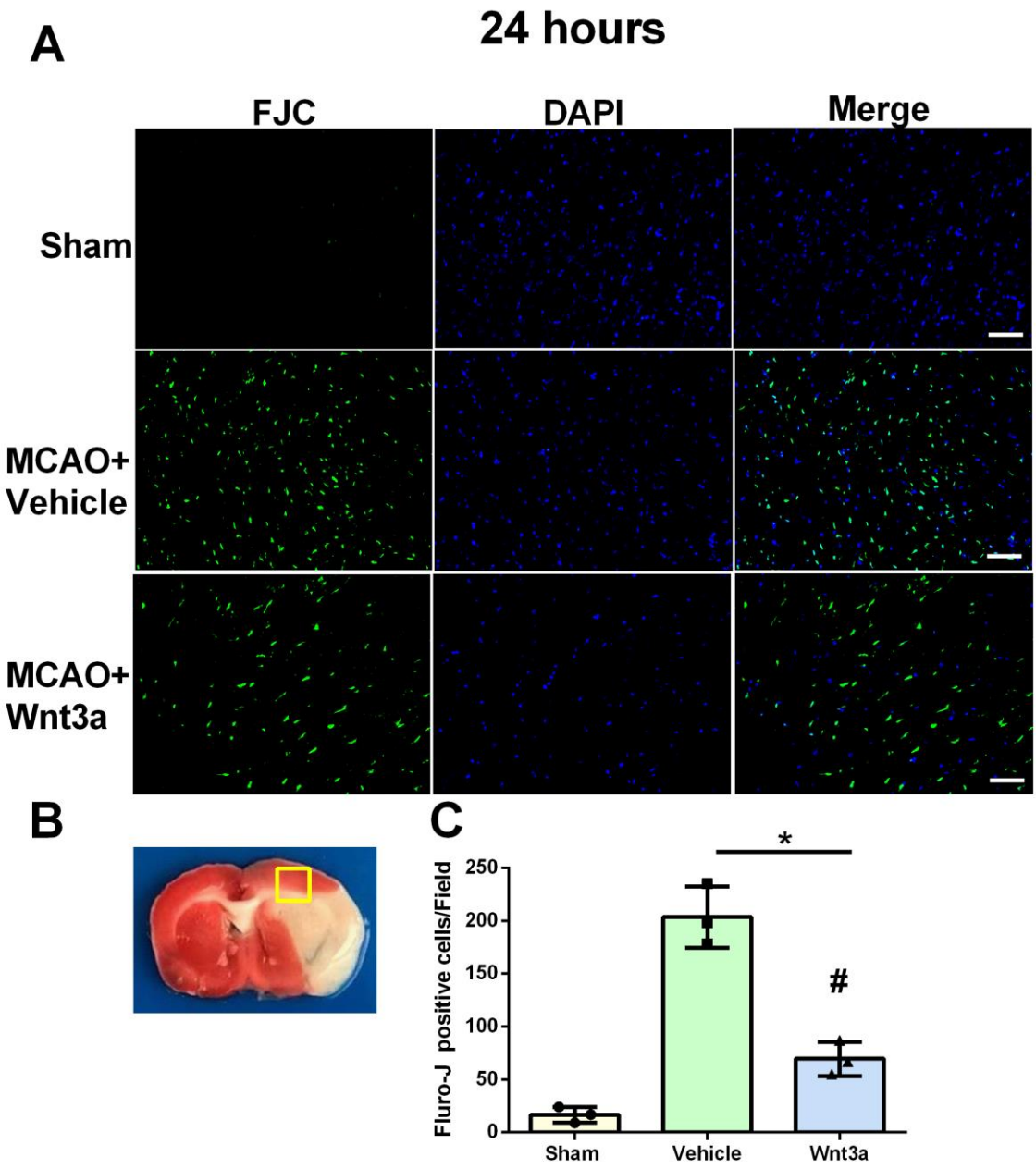

Figure 4. The effects of wnt3a on neuronal damage at 24 h after MCAO. (A) Representative microphotographs of Fluoro-Jade C staining (FJC)-positive neurons. (B) Quantitative analysis of JFC-positive cells was performed in the penumbra of the cortex. (C) FJC-positive neurons significantly increased after MCAO induction. Wnt3a significantly reduced the number of FJC-positive cells compared with vehicle ($p<0.05$). Data was presented as mean ±SD. Scale bar = 50 µm, n=3 per group. *$p<0.05$ vs. Sham, #$p<0.05$ vs vehicle.

Immunofluorescence of the Receptor Frz1 in the Penumbra at 24 h

Staining at the edge of the infarction (Fig. 5A) at 24 h probed neurons (NeuN), astrocytes (GFAP), and microglia (Iba1). In the sham group, immunoreactivity of Frz1 (red) was present in NeuN and GFAP, but not Iba-1 (Fig. 5B). Vehicle expression of Frz1 in Neun, GFAP, or Iba-1 could not be detected after MCAO. HD wnt3a treatment (1.2 µg/kg) demonstrated strong immunoreactivity of Frz1 colocalized with NeuN (Fig. 5B). Although literature agrees with Iba-1 expression on microglial cells, our observations suggest that the expression of Frz1 on Iba-1 may need to be evaluated at later time-points, peaking from 72h to 7days after MCAO (Michalski *et al.*, 2012; Kawabori *et al.*, 2015; Taylor & Sansing, 2013).

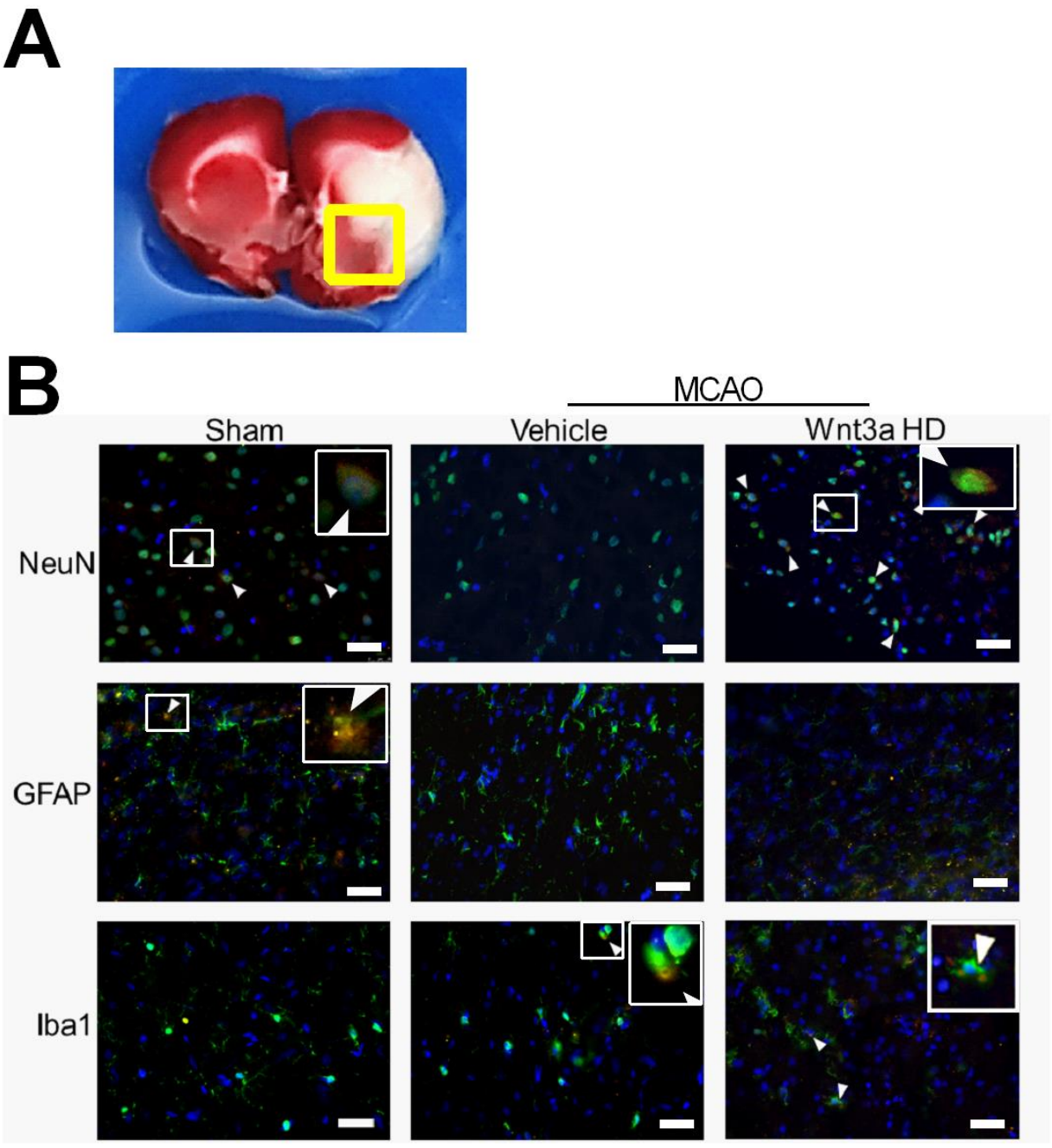

Figure 5. Expression of Frz1 (red) in neurons (NeuN, green), astrocytes (GFAP, green), and microglia (Iba1, green) in sham, vehicle, and treatment. Expression of Frz1 decreased in vehicle at 24 HR after MCAO in neurons but was increased with treatment. Sham showed minimal expression of Frz1 in astrocytes but no expression in microglia; however, vehicle and HD treatment (1.2 µg/kg) had no Frz1 expression in astrocytes, but minimal expression in microglia (n=1 per each group). DAPI (blue) indicates 4′,6-diamidino-2-phenylindole, dihydrochloride. Scale bar: 50µm.

Effects of wnt3a on Frz1, p-GSK3β, β-catenin, PIWI1a, FOXM1, CC-3 Pathway at 24 h and 72 h after MCAO

Of particular interest, recent studies have shown activation of extrinsic and intrinsic pathways of caspase-mediated cell death in several forms of transient MCAO in adult rats (Ferrer & Planas, 2003). Cleaved-caspase-3 is upregulated following MCAO, and subsequently, the inhibition of caspase-3 reduces infarct size following transient MCAO (Ferrer & Planas, 2003). Thus, our hypothesis is that wnt3a will provide therapeutic benefits following ischemic stroke in rats via attenuation of cleaved-caspase-3 and prevention of neuronal apoptosis. To investigate the effects of Frz1 activation with the specific HD wnt3a (1.2 µg/kg) agonist administered intranasally (iN) at one hour after reperfusion, western blot was performed on the right-hemisphere of the brain, representative images in Fig 6A. In the 24 h MCAO + vehicle group the proteins: wnt3a, Frz1, PIWI1a, and FOXM1 were significantly decreased compared to sham group ($p<0.05$; Fig 6B, C, D, G), while p-GSK3β and CC-3 were significantly increased compared to the sham group ($p<0.05$; Fig 6E, H). Additionally, at 24 h, HD wnt3a (1.2 µg/kg) iN treatment after MCAO significantly up-regulated the expression of Frz1, β-catenin, PIWI1a, and FOXM1 compared to vehicle groups ($p<0.05$; Fig 6B-D, F, G), while p-GSK3β and CC-3 were significantly attenuated compared to the vehicle group ($p<0.05$; Fig 6E, H). The 72 h MCAO + vehicle group wnt3a, Frz1, and FOXM1 were significantly decreased compared to sham ($p<0.05$; Fig 6B, C, G), while p-GSK3β, β-catenin, and CC-3 were significantly increased compared to the sham group ($p<0.05$; Fig 6E, F, H). In the 72 h MCAO + iN wnt3a (1.2 µg/kg) group, wnt3a, Frz1, β-catenin, and FOXM1 levels were significantly increased compared to vehicle groups ($p<0.05$; Fig 6B,

C, F, G); there was no change in PIWI1a levels at 72 h. Wnt3a expression was higher in vehicle groups at 24 and 72 h compared to endogenous expression levels after MCAO in Fig. 2B, which could be explained by two key observations. First, with a sample size of 4 in Fig 2B, the protein expression levels provided statistical significance to merit further mechanistic investigation into the significance of the pathway. Nonetheless, there still remains an opportunity for rather marked variation among small sample sizes despite statistically significant comparisons. With an increased sample size of 6, a more quantitative evaluation of the model and wnt3a expression could be observed. Second, the vehicle solution may have slightly increased the expression of endogenous wnt3a, but this expression was still significantly lower compared to sham. Additionally, iN wnt3a (1.2 μg/kg) significantly decreased levels of p-GSK3β, and CC-3 compared to the vehicle group ($p<0.05$; Fig 6E, H). Extended Fig. 6-1 reports the specific statistics for each group comparison.

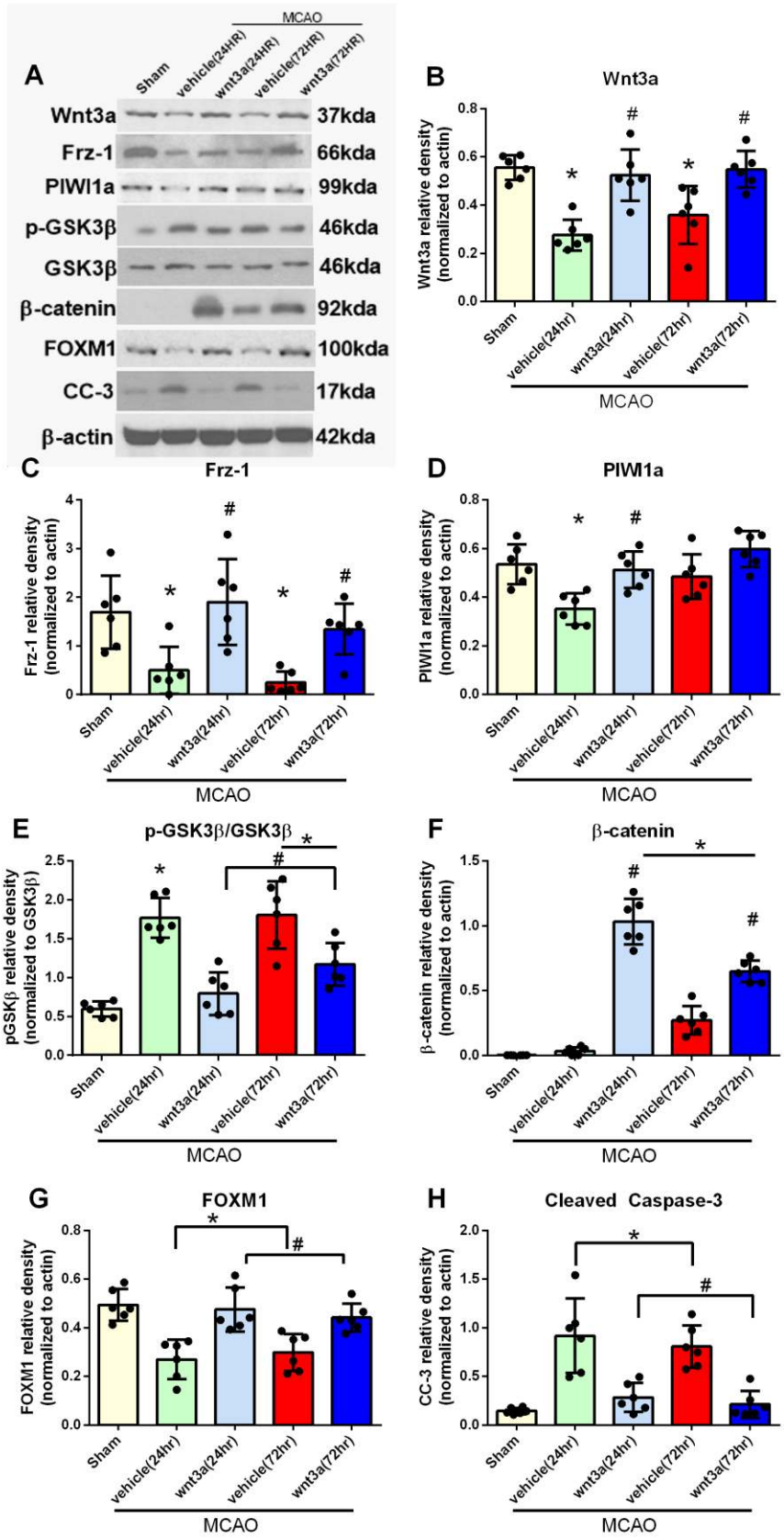
A
MCAO
Sham
vehicle(24HR)
wnt3a(24HR)
vehicle(72HR)
wnt3a(72HR)
Wnt3a 37kda
Frz-1 66kda
PIWI1a 99kda
p-GSK3β 46kda
GSK3β 46kda
β-catenin 92kda
FOXM1 100kda
CC-3 17kda
β-actin 42kda
B
Wnt3a
Wnt3a relative density (normalized to actin)
C
Frz-1
Frz-1 relative density (normalized to actin)
D
PIWI1a
PIWI1a relative density (normalized to actin)
E
p-GSK3β/GSK3β
pGSKβ relative density (normalized to GSK3β)
F
β-catenin
β-catenin relative density (normalized to actin)
G
FOXM1
FOXM1 relative density (normalized to actin)
H
Cleaved Caspase-3
CC-3 relative density (normalized to actin)
Sham
vehicle(24hr)
wnt3a(24hr)
vehicle(72hr)
wnt3a(72hr)
MCAO

Figure 6. Wnt3a prevented apoptosis through Frz1/PIWI1a/ β-catenin /FOXM1 pathway after MCAO in rats. (A) Right hemisphere representative Western blots of the rat brain. Wnt3a (B) and Frz1 (C) were increased after HD treatment (1.2 μg/kg) in both 24HR and 72HR endpoints. (D) PIWI1a was increased by wnt3a at 24HR but not lost its significance at 72HR. (E) pGsk-3β was increased in vehicle groups but reduced by the wnt3a treatment. (F) β-catenin was increased by wnt3a at both time points. (G) FOXM1 was brought back to sham levels by HD wnt3a treatment and (H) CC-3 was therefore reversed in the treatment groups. Each column represents the mean ± SD (n=6/group). *$p<0.05$ vs. Sham, #$p<0.05$ vs vehicle. Extended Fig. 6-1 reports the specific statistics for each group comparison

A

Treatment					
	Tukey's multiple comparisons test	Mean Diff.	95% CI of diff.	DF	p- value
wnt3a	Sham vs. vehicle(24hr)	0.2799	0.1315 to 0.4284	25	< 0.0001
	Sham vs. wnt3a(24hr)	0.03098	-0.1175 to 0.1795	25	0.9717
	Sham vs. vehicle(72hr)	0.1964	0.04795 to 0.3449	25	0.0055
	Sham vs. wnt3a(72hr)	0.007396	-0.1411 to 0.1559	25	0.9999
	vehicle(24hr) vs. wnt3a(24hr)	-0.249	-0.3974 to -0.1005	25	0.0004
	vehicle(24hr) vs. vehicle(72hr)	-0.08351	-0.2320 to 0.06496	25	0.4801
	vehicle(24hr) vs. wnt3a(72hr)	-0.2725	-0.4210 to -0.1241	25	0.0001
	wnt3a(24hr) vs. vehicle(72hr)	0.1655	0.01697 to 0.3139	25	0.0236
	wnt3a(24hr) vs. wnt3a(72hr)	-0.02358	-0.1721 to 0.1249	25	0.9897
	vehicle(72hr) vs. wnt3a(72hr)	-0.189	-0.3375 to -0.04055	25	0.0078
Frz1	Sham vs. vehicle(24hr)	1.194	0.1495 to 2.239	25	0.0194
	Sham vs. wnt3a(24hr)	-0.2051	-1.250 to 0.8399	25	0.9773
	Sham vs. vehicle(72hr)	1.445	0.4003 to 2.490	25	0.0035
	Sham vs. wnt3a(72hr)	0.3511	-0.6938 to 1.396	25	0.8587
	vehicle(24hr) vs. wnt3a(24hr)	-1.4	-2.444 to -0.3546	25	0.0049
	vehicle(24hr) vs. vehicle(72hr)	0.2508	-0.7941 to 1.296	25	0.9534
	vehicle(24hr) vs. wnt3a(72hr)	-0.8433	-1.888 to 0.2017	25	0.1568
	wnt3a(24hr) vs. vehicle(72hr)	1.65	0.6054 to 2.695	25	0.0008
	wnt3a(24hr) vs. wnt3a(72hr)	0.5562	-0.4887 to 1.601	25	0.5332
	vehicle(72hr) vs. wnt3a(72hr)	-1.094	-2.139 to -0.04914	25	0.0369
PIWI1a	Sham vs. vehicle(24hr)	0.1833	0.05089 to 0.3158	25	0.0035
	Sham vs. wnt3a(24hr)	0.0226	-0.1099 to 0.1551	25	0.9865
	Sham vs. vehicle(72hr)	0.05081	-0.08165 to 0.1833	25	0.7911
	Sham vs. wnt3a(72hr)	-0.06217	-0.1946 to 0.07029	25	0.6465
	vehicle(24hr) vs. wnt3a(24hr)	-0.1607	-0.2932 to -0.02829	25	0.0119
	vehicle(24hr) vs. vehicle(72hr)	-0.1325	-0.2650 to -7.921e-005	25	0.0498
	vehicle(24hr) vs. wnt3a(72hr)	-0.2455	-0.3780 to -0.1131	25	0.0001
	wnt3a(24hr) vs. vehicle(72hr)	0.02821	-0.1042 to 0.1607	25	0.9695
	wnt3a(24hr) vs. wnt3a(72hr)	-0.08477	-0.2172 to 0.04769	25	0.3537
	vehicle(72hr) vs. wnt3a(72hr)	-0.113	-0.2454 to 0.01948	25	0.1216
β-catenin	Sham vs. vehicle(24hr)	-0.03212	-0.2027 to 0.1385	25	0.9805
	Sham vs. wnt3a(24hr)	-1.03	-1.201 to -0.8594	25	< 0.0001
	Sham vs. vehicle(72hr)	-0.2692	-0.4398 to -0.09863	25	0.0008
	Sham vs. wnt3a(72hr)	-0.6466	-0.8172 to -0.4760	25	< 0.0001
	vehicle(24hr) vs. wnt3a(24hr)	-0.9979	-1.169 to -0.8273	25	< 0.0001
	vehicle(24hr) vs. vehicle(72hr)	-0.2371	-0.4077 to -0.06651	25	0.0034
	vehicle(24hr) vs. wnt3a(72hr)	-0.6145	-0.7851 to -0.4439	25	< 0.0001
	wnt3a(24hr) vs. vehicle(72hr)	0.7608	0.5902 to 0.9314	25	< 0.0001
	wnt3a(24hr) vs. wnt3a(72hr)	0.3834	0.2128 to 0.5540	25	< 0.0001
	vehicle(72hr) vs. wnt3a(72hr)	-0.3774	-0.5480 to -0.2068	25	< 0.0001
p-GSK3β/GSK3β	Sham vs. vehicle(24hr)	-0.6741	-0.9761 to -0.3721	25	< 0.0001
	Sham vs. wnt3a(24hr)	-0.2677	-0.5697 to 0.03424	25	0.7533
	Sham vs. vehicle(72hr)	-0.6652	-0.9671 to -0.3632	25	< 0.0001
	Sham vs. wnt3a(72hr)	-0.3476	-0.6496 to -0.04565	25	0.0149

B

	vehicle(24hr) vs. wnt3a(24hr)	0.4064	0.1044 to 0.7084	25	< 0.0001
	vehicle(24hr) vs. vehicle(72hr)	0.008948	-0.2930 to 0.3109	25	0.9995
	vehicle(24hr) vs. wnt3a(72hr)	0.3265	0.02453 to 0.6285	25	0.0107
	wnt3a(24hr) vs. vehicle(72hr)	-0.3974	-0.6994 to -0.09547	25	< 0.0001
	wnt3a(24hr) vs. wnt3a(72hr)	-0.07989	-0.3819 to 0.2221	25	0.1872
	vehicle(72hr) vs. wnt3a(72hr)	0.3175	0.01558 to 0.6195	25	0.0064
FOXM1	Sham vs. vehicle(24hr)	0.2251	0.09803 to 0.3522	25	0.0002
	Sham vs. wnt3a(24hr)	0.01897	-0.1081 to 0.1460	25	0.9918
	Sham vs. vehicle(72hr)	0.1956	0.06855 to 0.3227	25	0.0011
	Sham vs. wnt3a(72hr)	0.05304	-0.07402 to 0.1801	25	0.7366
	vehicle(24hr) vs. wnt3a(24hr)	-0.2061	-0.3332 to -0.07907	25	0.0006
	vehicle(24hr) vs. vehicle(72hr)	-0.02948	-0.1565 to 0.09758	25	0.9587
	vehicle(24hr) vs. wnt3a(72hr)	-0.1721	-0.2991 to -0.04499	25	0.0044
	wnt3a(24hr) vs. vehicle(72hr)	0.1766	0.04958 to 0.3037	25	0.0034
	wnt3a(24hr) vs. wnt3a(72hr)	0.03407	-0.09299 to 0.1611	25	0.9318
	vehicle(72hr) vs. wnt3a(72hr)	-0.1426	-0.2696 to -0.01551	25	0.0224
CC-3	Sham vs. vehicle(24hr)	-0.7731	-1.142 to -0.4038	25	< 0.0001
	Sham vs. wnt3a(24hr)	-0.1396	-0.5089 to 0.2297	25	0.7995
	Sham vs. vehicle(72hr)	-0.6626	-1.032 to -0.2933	25	0.0002
	Sham vs. wnt3a(72hr)	-0.06812	-0.4374 to 0.3012	25	0.982
	vehicle(24hr) vs. wnt3a(24hr)	0.6335	0.2642 to 1.003	25	0.0003
	vehicle(24hr) vs. vehicle(72hr)	0.1106	-0.2587 to 0.4799	25	0.9018
	vehicle(24hr) vs. wnt3a(72hr)	0.705	0.3357 to 1.074	25	< 0.0001
	wnt3a(24hr) vs. vehicle(72hr)	-0.5229	-0.8922 to -0.1536	25	0.0028
	wnt3a(24hr) vs. wnt3a(72hr)	0.07152	-0.2978 to 0.4408	25	0.9784
	vehicle(72hr) vs. wnt3a(72hr)	0.5944	0.2251 to 0.9637	25	0.0007

Table 6-1. P values from each comparison in treatment study looking at 24hr and 72hr endpoints (Figure 6). One-way ANOVA with Tukey's multiple comparisons tests were run on western blot groups and the mean differences shown (n=6/group). *p<.05, **p<0.01, ***p<0.001, ****p<0.0001.

Effects of wnt3a on Infarct Size and Neurobehavioral Function 72 h after MCAO

To evaluate the effects of iN wnt3a high dose (1.2 ug/kg) on long-term neurological outcome, infarct and neurobehavior were assessed at 72 h. With administration of wnt3a, infarction volume was significantly reduced compared to vehicle (One-way ANOVA; Tukey's test; $F(2, 15) = 25.20$; $n=6$; $p=0.0084$) (Fig 7A). Wnt3a restored modified Garcia (Fig 7B), left-forelimb placement (Fig 7C), and corner-turn (Fig 7D) scores to sham levels. In the 72 h MCAO + vehicle group, infarction volume was significantly increased and neurobehavior scores for: modified Garcia (One-way ANOVA; Kruskal-Wallis with Dunn's post-hoc; $p=0.023$; Fig 7B), left-forelimb placement (One-way ANOVA; Tukey's test; $F(2, 15) = 8.59$; $n=6$; $p=0.003$; Fig 7C), and corner-turn (One-way ANOVA; Tukey's test; $F(2, 15) = 5.86$; $n=6$; $p=0.0102$; Fig 7D) were significantly decreased compared to sham.

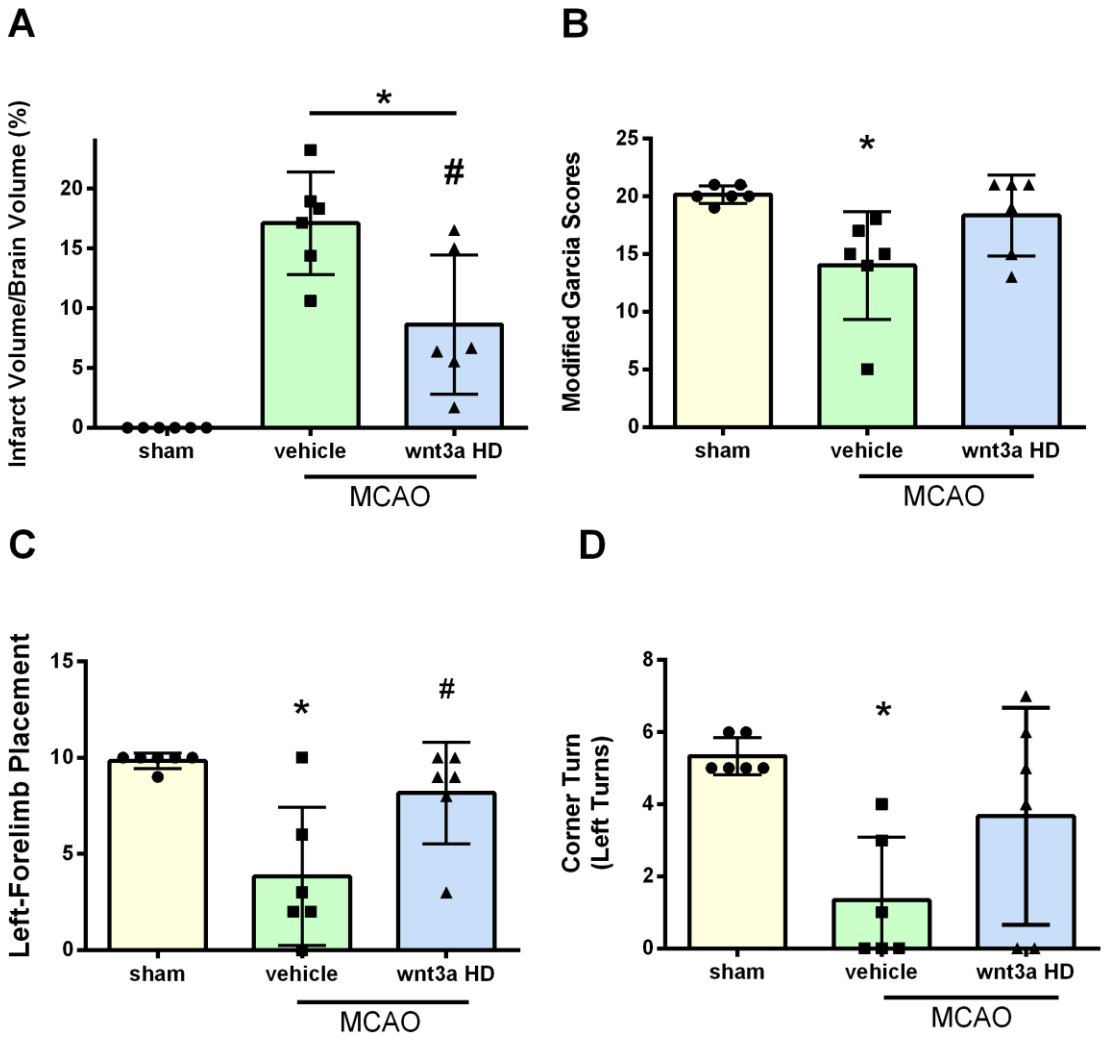

Figure 7. Wnt3a decreased infarct volume (A) and improved neurological function 72 hours after MCAO. (B) Cerebral infarct quantification was carried out on the TTC stained images of coronal sections, (C) modified Garcia neuroscore, (D) left-forelimb placement, (E) corner turn test showed that high dosage of Wnt3a decreases infarction and neurological deficits 72 hours after MCAO. Each column represents the mean ± SD (n=6/group). *p<0.05 vs. Sham, #p<0.05 vs vehicle.

Impact of Frz1-siRNA, PIWI1a-siRNA and PIWI CRISPR on the Function of the wnt3a/Frz1/PIWI/FOXM1 Pathway at 24 h after MCAO

To elucidate the molecular mechanisms modulated by wnt3a downstream of its receptor Frz1, two inhibitor groups were used, Frz1-siRNA and PIWI siRNA. At 24 h, MCAO+wnt3a+Frz1-siRNA significantly decreased the protein expression of wnt3a, Frz1, PIWI1a, and FOXM1 compared to the wnt3a treated group ($p<0.05$; Fig 8B-D, F); pGSK3β, and CC-3 were significantly increased compared to the wnt3a treated and scrambled control groups ($p<0.05$; Fig 8E, G). In the MCAO+wnt3a+PIWI siRNA group, Frz1, PIWI1a, and FOXM1 were significantly decreased compared to the treated and scramble control groups ($p<0.05$; Fig 8C, D, F); wnt3a, pGSK3β, and CC-3 were significantly increased compared to the treated and scramble control groups ($p<0.05$; Fig 8B, E, G). In the MCAO+wnt3a+Frz1-siRNA+PIWI CRISPR group, protein expression of PIWI1a and FOXM1 was significantly increased compared to vehicle group ($p<0.05$; Fig 8D, F); wnt3a, Frz1, pGSK3β, and CC-3 were significantly decreased compared to wnt3a treated group ($p<0.05$; Fig 8B, C, E, G). Extended Fig 8-1 reports the specific statistics for each group comparison.

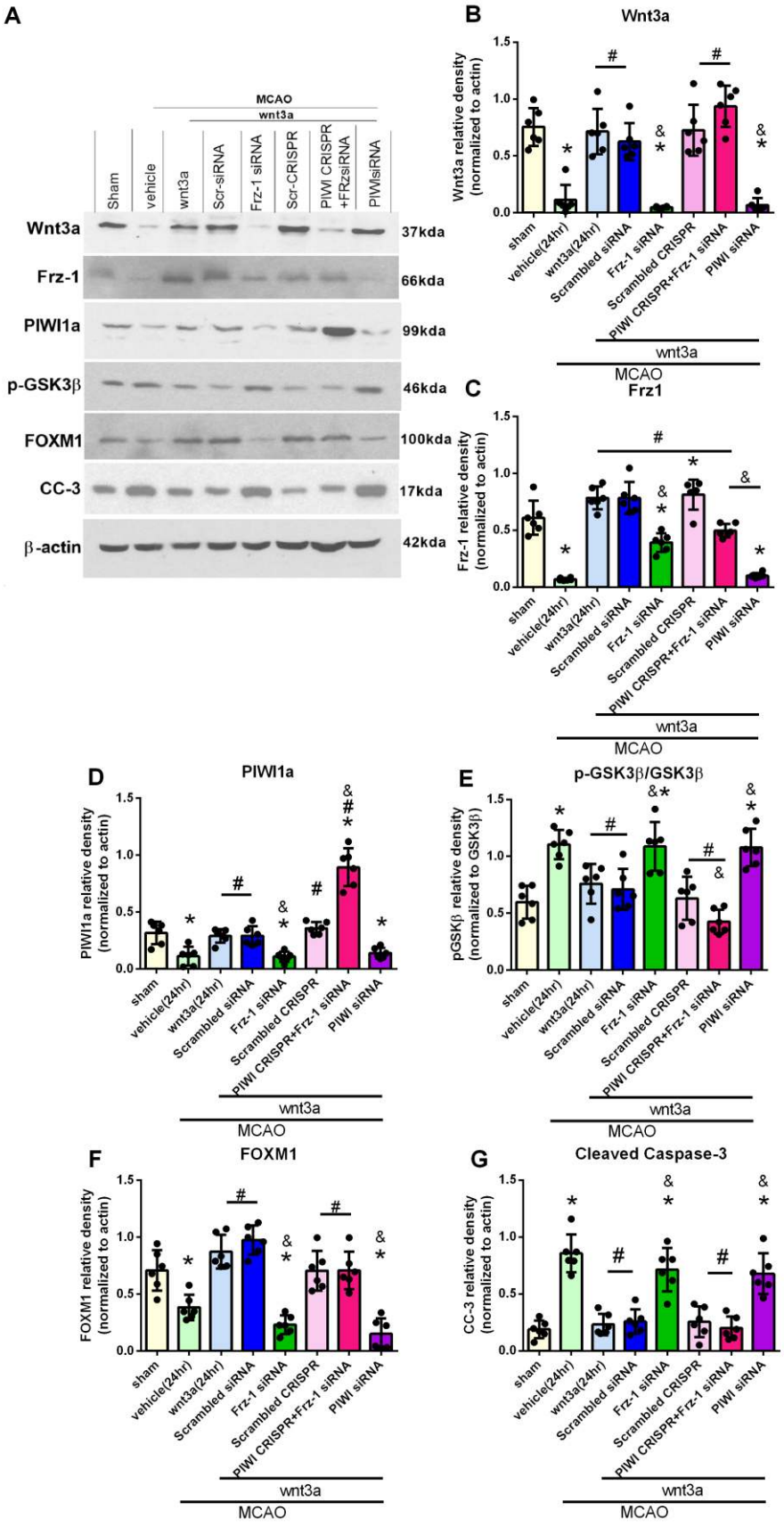
A
MCAO
wnt3a
Sham
vehicle
wnt3a
Scr-siRNA
Frz-1 siRNA
Scr-CRISPR
PIWI CRISPR +FRzsiRNA
PIWIsiRNA
Wnt3a
37kda
Frz-1
66kda
PIWI1a
99kda
p-GSK3β
46kda
FOXM1
100kda
CC-3
17kda
β-actin
42kda
B
Wnt3a
Wnt3a relative density (normalized to actin)
C
Frz1
Frz-1 relative density (normalized to actin)
D
PIWI1a
PIWI1a relative density (normalized to actin)
E
p-GSK3β/GSK3β
pGSKβ relative density (normalized to GSK3β)
F
FOXM1
FOXM1 relative density (normalized to actin)
G
Cleaved Caspase-3
CC-3 relative density (normalized to actin)
sham
vehicle(24hr)
wnt3a(24hr)
Scrambled siRNA
Frz-1 siRNA
Scrambled CRISPR
PIWI CRISPR+Frz-1 siRNA
PIWI siRNA
wnt3a
MCAO

Figure 8. Effect of Wnt3a preventing apoptosis through the Frz1/PIWI1a/FOXM1 pathway at 24Hr after MCAO. (A) Right hemisphere representative Western blots of the rat brain for the pathway. (B) After siRNA treatment of Frz1, Wnt3a returned to vehicle levels and (C) Frz1 expression was dependent on the presence of wnt3a, which was significantly reduced with Frz1-siRNA and PIWI-siRNA. With the increased expression of PIWI1a (D) through treatment or CRISPR, pGsk-3β (E) was decreased. (F) FOXM1 was increased in expression through treatment and decreased through Frz1-siRNA and PIWI-siRNA. (G) CC3 was decreased after treatment but restored to vehicle levels by the inhibition of the Frz1/PIWI1a/FOXM1 pathway with both Frz1-siRNA and PIWI-siRNA. Each column represents the mean ± SD (n=6/group). *$p<0.05$ vs. Sham, #$p<0.05$ vs. vehicle, &$p<0.05$ vs. wnt3a. Extended Fig. 8-1 reports the specific statistics for each group comparison.

A

Interventions					
	Tukey's Comparison Test	Mean Diff.	95% CI of diff.	DF	p- value
wnt3a	sham vs. vehicle(24hr)	0.6412	0.3500 to 0.9323	40	< 0.0001
	sham vs. wnt3a(24hr)	0.03933	-0.2518 to 0.3305	40	0.9998
	sham vs. Scrambled siRNA	0.1283	-0.1629 to 0.4195	40	0.848
	sham vs. Frz-1 siRNA	0.7061	0.4150 to 0.9973	40	< 0.0001
	sham vs. Scrambled CRISPR	0.02674	-0.2644 to 0.3179	40	> 0.9999
	sham vs. PIWI CRISPR+Frz-1 siRNA	-0.1825	-0.4736 to 0.1087	40	0.4925
	sham vs. PIWI siRNA	0.6847	0.3936 to 0.9759	40	< 0.0001
	vehicle(24hr) vs. wnt3a(24hr)	-0.6019	-0.8930 to -0.3107	40	< 0.0001
	vehicle(24hr) vs. Scrambled siRNA	-0.5129	-0.8040 to -0.2217	40	< 0.0001
	vehicle(24hr) vs. Frz-1 siRNA	0.06493	-0.2262 to 0.3561	40	0.9961
	vehicle(24hr) vs. Scrambled CRISPR	-0.6144	-0.9056 to -0.3233	40	< 0.0001
	vehicle(24hr) vs. PIWI CRISPR+Frz-1 siRNA	-0.8237	-1.115 to -0.5325	40	< 0.0001
	vehicle(24hr) vs. PIWI siRNA	0.04353	-0.2476 to 0.3347	40	0.9997
	wnt3a(24hr) vs. Scrambled siRNA	0.08897	-0.2022 to 0.3801	40	0.9752
	wnt3a(24hr) vs. Frz-1 siRNA	0.6668	0.3756 to 0.9579	40	< 0.0001
	wnt3a(24hr) vs. Scrambled CRISPR	-0.01259	-0.3037 to 0.2786	40	> 0.9999
	wnt3a(24hr) vs. PIWI CRISPR+Frz-1 siRNA	-0.2218	-0.5130 to 0.06936	40	0.253
	wnt3a(24hr) vs. PIWI siRNA	0.6454	0.3542 to 0.9365	40	< 0.0001
Frz1	sham vs. vehicle(24hr)	0.5411	0.3561 to 0.7260	40	< 0.0001
	sham vs. wnt3a(24hr)	-0.1752	-0.3602 to 0.009789	40	0.0747
	sham vs. Scrambled siRNA	-0.1752	-0.3601 to 0.009831	40	0.0748
	sham vs. Frz-1 siRNA	0.218	0.03307 to 0.4030	40	0.0113
	sham vs. Scrambled CRISPR	-0.2033	-0.3883 to -0.01836	40	0.0224
	sham vs. PIWI CRISPR+Frz-1 siRNA	0.1134	-0.07154 to 0.2984	40	0.5199
	sham vs. PIWI siRNA	0.5088	0.3238 to 0.6938	40	< 0.0001
	vehicle(24hr) vs. wnt3a(24hr)	-0.7163	-0.9012 to -0.5313	40	< 0.0001
	vehicle(24hr) vs. Scrambled siRNA	-0.7162	-0.9012 to -0.5312	40	< 0.0001
	vehicle(24hr) vs. Frz-1 siRNA	-0.323	-0.5080 to -0.1380	40	< 0.0001
	vehicle(24hr) vs. Scrambled CRISPR	-0.7444	-0.9294 to -0.5594	40	< 0.0001
	vehicle(24hr) vs. PIWI CRISPR+Frz-1 siRNA	-0.4276	-0.6126 to -0.2426	40	< 0.0001
	vehicle(24hr) vs. PIWI siRNA	-0.03224	-0.2172 to 0.1527	40	0.9992
	wnt3a(24hr) vs. Scrambled siRNA	4.20E-05	-0.1849 to 0.1850	40	> 0.9999
	wnt3a(24hr) vs. Frz-1 siRNA	0.3932	0.2083 to 0.5782	40	< 0.0001
	wnt3a(24hr) vs. Scrambled CRISPR	-0.02815	-0.2131 to 0.1568	40	0.9997
	wnt3a(24hr) vs. PIWI CRISPR+Frz-1 siRNA	0.2886	0.1037 to 0.4736	40	0.0003
	wnt3a(24hr) vs. PIWI siRNA	0.684	0.4990 to 0.8690	40	< 0.0001
PIWI1a	sham vs. vehicle(24hr)	0.2053	0.04305 to 0.3674	40	0.0052
	sham vs. wnt3a(24hr)	0.02771	-0.1345 to 0.1899	40	0.9993
	sham vs. Scrambled siRNA	0.02629	-0.1359 to 0.1885	40	0.9995
	sham vs. Frz-1 siRNA	0.2089	0.04668 to 0.3711	40	0.0042
	sham vs. Scrambled CRISPR	-0.04035	-0.2025 to 0.1218	40	0.9924
	sham vs. PIWI CRISPR+Frz-1 siRNA	-0.5773	-0.7395 to -0.4151	40	< 0.0001
	sham vs. PIWI siRNA	0.1772	0.01501 to 0.3394	40	0.0237
	vehicle(24hr) vs. wnt3a(24hr)	-0.1775	-0.3397 to -0.01535	40	0.0233

B

	vehicle(24hr) vs. Scrambled siRNA	-0.179	-0.3412 to -0.01676	40	0.0217
	vehicle(24hr) vs. Frz-1 siRNA	0.003623	-0.1586 to 0.1658	40	> 0.9999
	vehicle(24hr) vs. Scrambled CRISPR	-0.2456	-0.4078 to -0.08340	40	0.0005
	vehicle(24hr) vs. PIWI CRISPR+Frz-1 siRNA	-0.7825	-0.9447 to -0.6203	40	< 0.0001
	vehicle(24hr) vs. PIWI siRNA	-0.02805	-0.1902 to 0.1341	40	0.9992
	wnt3a(24hr) vs. Scrambled siRNA	-0.001415	-0.1636 to 0.1608	40	> 0.9999
	wnt3a(24hr) vs. Frz-1 siRNA	0.1812	0.01897 to 0.3434	40	0.0193
	wnt3a(24hr) vs. Scrambled CRISPR	-0.06805	-0.2302 to 0.09414	40	0.8773
	wnt3a(24hr) vs. PIWI CRISPR+Frz-1 siRNA	-0.605	-0.7672 to -0.4428	40	< 0.0001
	wnt3a(24hr) vs. PIWI siRNA	0.1495	-0.01270 to 0.3117	40	0.0898
p-GSK3β/GSK3β	sham vs. vehicle(24hr)	-0.4667	-0.7302 to -0.2031	40	0.0001
	sham vs. wnt3a(24hr)	-0.09372	-0.3573 to 0.1698	40	0.6812
	sham vs. Scrambled siRNA	-0.06512	-0.3287 to 0.1984	40	0.9312
	sham vs. Frz-1 siRNA	-0.4158	-0.6794 to -0.1523	40	0.0002
	sham vs. Scrambled CRISPR	-0.07126	-0.3348 to 0.1923	40	> 0.9999
	sham vs. PIWI CRISPR+Frz-1 siRNA	0.004671	-0.2589 to 0.2682	40	0.6292
	sham vs. PIWI siRNA	-0.3921	-0.6556 to -0.1286	40	0.0003
	vehicle(24hr) vs. wnt3a(24hr)	0.3729	0.1094 to 0.6365	40	0.0177
	vehicle(24hr) vs. Scrambled siRNA	0.4015	0.1380 to 0.6651	40	0.0041
	vehicle(24hr) vs. Frz-1 siRNA	0.05085	-0.2127 to 0.3144	40	> 0.9999
	vehicle(24hr) vs. Scrambled CRISPR	0.3954	0.1319 to 0.6589	40	0.0003
	vehicle(24hr) vs. PIWI CRISPR+Frz-1 siRNA	0.4713	0.2078 to 0.7349	40	< 0.0001
	vehicle(24hr) vs. PIWI siRNA	0.07456	-0.1890 to 0.3381	40	> 0.9999
	wnt3a(24hr) vs. Scrambled siRNA	0.0286	-0.2349 to 0.2921	40	0.9995
	wnt3a(24hr) vs. Frz-1 siRNA	-0.3221	-0.5856 to -0.05854	40	0.0282
	wnt3a(24hr) vs. Scrambled CRISPR	0.02246	-0.2411 to 0.2860	40	0.875
	wnt3a(24hr) vs. PIWI CRISPR+Frz-1 siRNA	0.09839	-0.1652 to 0.3619	40	0.0232
	wnt3a(24hr) vs. PIWI siRNA	-0.2984	-0.5619 to -0.03484	40	0.0365
FOXM1	sham vs. vehicle(24hr)	0.3268	0.06212 to 0.5914	40	0.0069
	sham vs. wnt3a(24hr)	-0.1625	-0.4271 to 0.1022	40	0.5186
	sham vs. Scrambled siRNA	-0.2645	-0.5291 to 0.0001765	40	0.0503
	sham vs. Frz-1 siRNA	0.4774	0.2127 to 0.7420	40	< 0.0001
	sham vs. Scrambled CRISPR	0.003951	-0.2607 to 0.2686	40	> 0.9999
	sham vs. PIWI CRISPR+Frz-1 siRNA	0.00141	-0.2632 to 0.2661	40	> 0.9999
	sham vs. PIWI siRNA	0.5573	0.2926 to 0.8219	40	< 0.0001
	vehicle(24hr) vs. wnt3a(24hr)	-0.4892	-0.7539 to -0.2246	40	< 0.0001
	vehicle(24hr) vs. Scrambled siRNA	-0.5912	-0.8559 to -0.3266	40	< 0.0001
	vehicle(24hr) vs. Frz-1 siRNA	0.1506	-0.1141 to 0.4152	40	0.6116
	vehicle(24hr) vs. Scrambled CRISPR	-0.3228	-0.5875 to -0.05817	40	0.0079
	vehicle(24hr) vs. PIWI CRISPR+Frz-1 siRNA	-0.3254	-0.5900 to -0.06071	40	0.0072
	vehicle(24hr) vs. PIWI siRNA	0.2305	-0.03416 to 0.4951	40	0.128
	wnt3a(24hr) vs. Scrambled siRNA	-0.102	-0.3667 to 0.1626	40	0.9173
	wnt3a(24hr) vs. Frz-1 siRNA	0.6398	0.3752 to 0.9045	40	< 0.0001
	wnt3a(24hr) vs. Scrambled CRISPR	0.1664	-0.09823 to 0.4311	40	0.4882
	wnt3a(24hr) vs. PIWI CRISPR+Frz-1 siRNA	0.1639	-0.1008 to 0.4285	40	0.5077
	wnt3a(24hr) vs. PIWI siRNA	0.7197	0.4551 to 0.9844	40	< 0.0001

C

CC-3	sham vs. vehicle(24hr)	-0.6681	-0.9214 to -0.4148	40	< 0.0001
	sham vs. wnt3a(24hr)	-0.04245	-0.2958 to 0.2109	40	0.9994
	sham vs. Scrambled siRNA	-0.06929	-0.3226 to 0.1840	40	0.9868
	sham vs. Frz-1 siRNA	-0.5247	-0.7780 to -0.2713	40	< 0.0001
	sham vs. Scrambled CRISPR	-0.06596	-0.3193 to 0.1874	40	0.9901
	sham vs. PIWI CRISPR+Frz-1 siRNA	-0.01154	-0.2649 to 0.2418	40	> 0.9999
	sham vs. PIWI siRNA	-0.4883	-0.7416 to -0.2350	40	< 0.0001
	vehicle(24hr) vs. wnt3a(24hr)	0.6256	0.3723 to 0.8790	40	< 0.0001
	vehicle(24hr) vs. Scrambled siRNA	0.5988	0.3455 to 0.8521	40	< 0.0001
	vehicle(24hr) vs. Frz-1 siRNA	0.1434	-0.1099 to 0.3968	40	0.6173
	vehicle(24hr) vs. Scrambled CRISPR	0.6021	0.3488 to 0.8555	40	< 0.0001
	vehicle(24hr) vs. PIWI CRISPR+Frz-1 siRNA	0.6566	0.4032 to 0.9099	40	< 0.0001
	vehicle(24hr) vs. PIWI siRNA	0.1798	-0.07353 to 0.4331	40	0.3354
	wnt3a(24hr) vs. Scrambled siRNA	-0.02684	-0.2802 to 0.2265	40	> 0.9999
	wnt3a(24hr) vs. Frz-1 siRNA	-0.4822	-0.7355 to -0.2289	40	< 0.0001
	wnt3a(24hr) vs. Scrambled CRISPR	-0.02351	-0.2768 to 0.2298	40	> 0.9999
	wnt3a(24hr) vs. PIWI CRISPR+Frz-1 siRNA	0.03091	-0.2224 to 0.2842	40	> 0.9999
	wnt3a(24hr) vs. PIWI siRNA	-0.4459	-0.6992 to -0.1926	40	< 0.0001

Table 8-1. P values from each comparison in the intervention pathway analysis (Figure 8). One-way ANOVA with Tukey's multiple comparisons tests were run on western blot groups and the mean differences shown (n=6/group). *p<.05, **p<0.01, ***p<0.001, ****p<0.0001.

Sexually Dimorphic Comparisons of Infarct Size and Neurobehavioral Function 24 h after MCAO in Female Rats

To evaluate for sexually dimorphic differences after treatment, infarct and neurobehavior were assessed at 24 h in female rats. With administration of wnt3a, infarction volume was significantly reduced compared to vehicle (One-way ANOVA; Tukey's test; $F(2, 15) = 53.11$; $n=6$, $p=0.0079$) (Fig 9B). Wnt3a restored modified Garcia (Fig 9C) and left-forelimb placement (Fig 9D) scores to sham levels. HD wnt3a (1.2 ug/kg) treatment after MCAO had significantly therapeutic effects in both sexes, with no major inter-sex differences in infarct and behavioral evaluations.

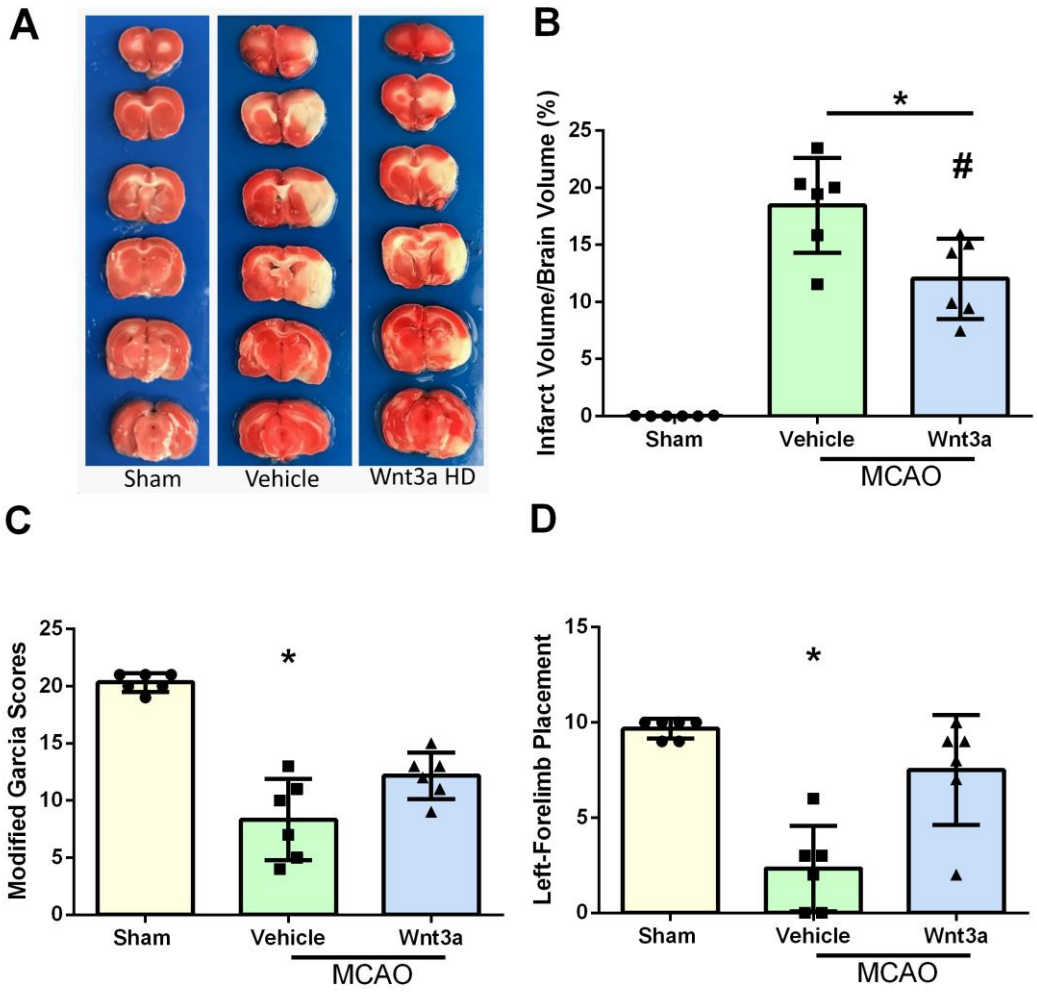

Figure 9. Wnt3a attenuated infarct volume and improved neurological function 24 hours after MCAO in female rats. (A) Representative TTC staining images of coronal sections in female rats. (B) Wnt3a HD effectively reduced the infarct volume. (C) Modified Garcia showed that wnt3a improved neurological function. (D) Left-forelimb placement was improved with wnt3a. Each column represents the mean ± SD (n=6/group). *p<0.05 vs. Sham, #p<0.05 vs vehicle.

Age-related Effects on Infarct Size and Neurobehavioral Function 24 h after MCAO

To assess the age-related effects after MCAO, neurological outcome, infarct and neurobehavior were assessed at 24 h in 9-month old aged male rats. With administration of wnt3a, infarction volume was significantly reduced compared to vehicle (One-way ANOVA; Tukey's test; F (2, 15) =115.8; n=6; p=0.0124) (Fig 10B). Wnt3a had no effect on Modified Garcia (Fig 10C), and both vehicle (One-way ANOVA; Kruskal-Wallis with Dunn's post-hoc; n=6; P=0.0053) and treatment (One-way ANOVA; Kruskal-Wallis with Dunn's post-hoc; n=6; P=0.0181) Modified Garcia scores were decreased compared to sham. Wnt3a restored left-forelimb placement (Fig 10D) scores to sham levels. Overall, HD wnt3a (1.2 ug/kg) treatment in aged rats was not as advantageous when compared to younger treated MCAO cohorts; however, significant reduction of infarction and improved Left-Forelimb placement was observed.

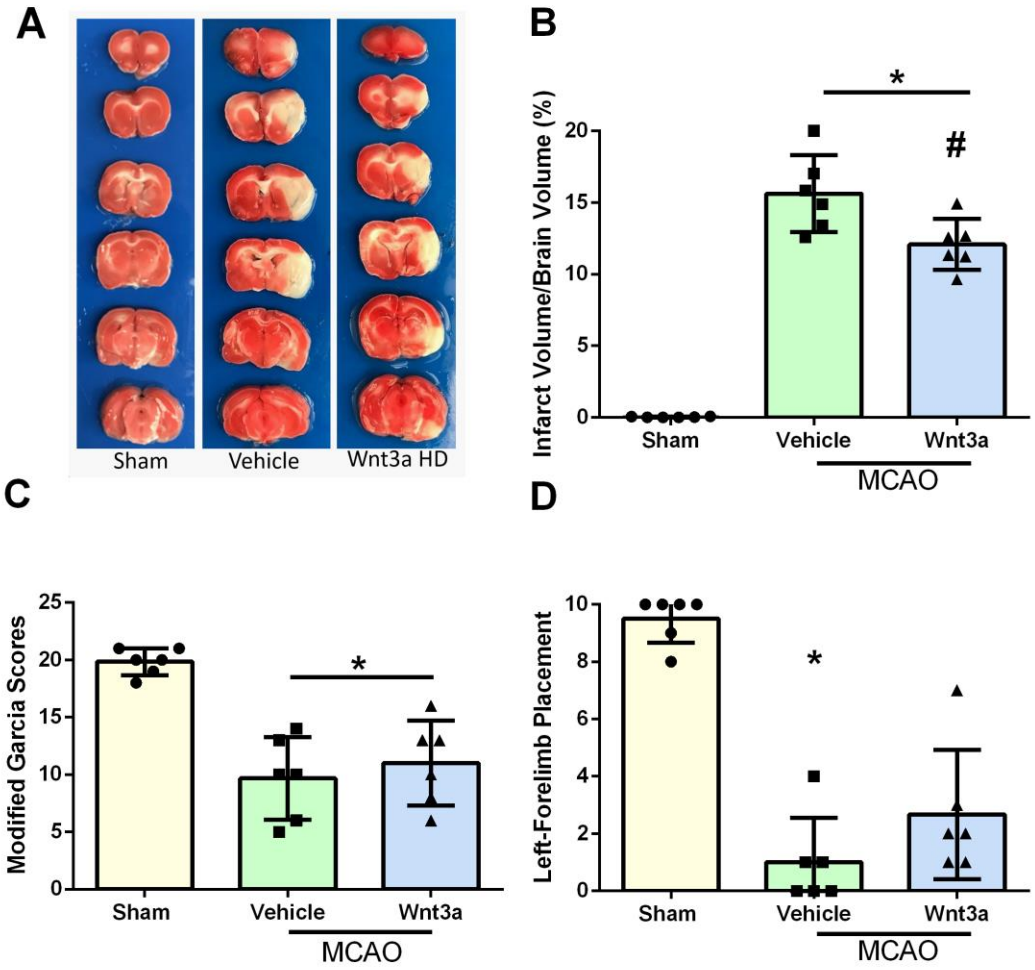

Figure 10. 9-month-old aged rats were evaluated at 24 hours after MCAO and showed a reduction in infarct volume with an improved Left-forelimb placement after wnt3a administration. (A) Representative TTC staining images of coronal sections in aged rats. (B) Wnt3a effectively reduced infarct volume compared to vehicle. (C) Modified Garcia was not able to detect an effect after wnt3a administration compared to vehicle. (D) Left-forelimb placement was improved with wnt3a. Each column represents the mean ± SD (n=6/group). *p<0.05 vs. Sham, #p<0.05 vs vehicle.

Wnt3a Effects on Infarct Size and Neurobehavioral Function at 24 h in a Permanent Middle Cerebral Artery Occlusion (pMCAO) Model

To evaluate the model variation effects on neurological outcome, infarct and neurobehavior were assessed at 24 h in a permanent middle cerebral artery occlusion (pMCAO) model. With administration of wnt3a, no significant improvement was seen in infarction compared to vehicle (One-way ANOVA; Tukey's test; $F(2, 15) = 59.35$; $n=6$, $p=0.8816$; Fig 11B). Both modified Garcia (Fig 11C) and left-forelimb (Fig 11D) placement showed no significant difference in treatment compared to vehicle (One-way ANOVA; Kruskal-Wallis with Dunn's post-hoc; n=6).

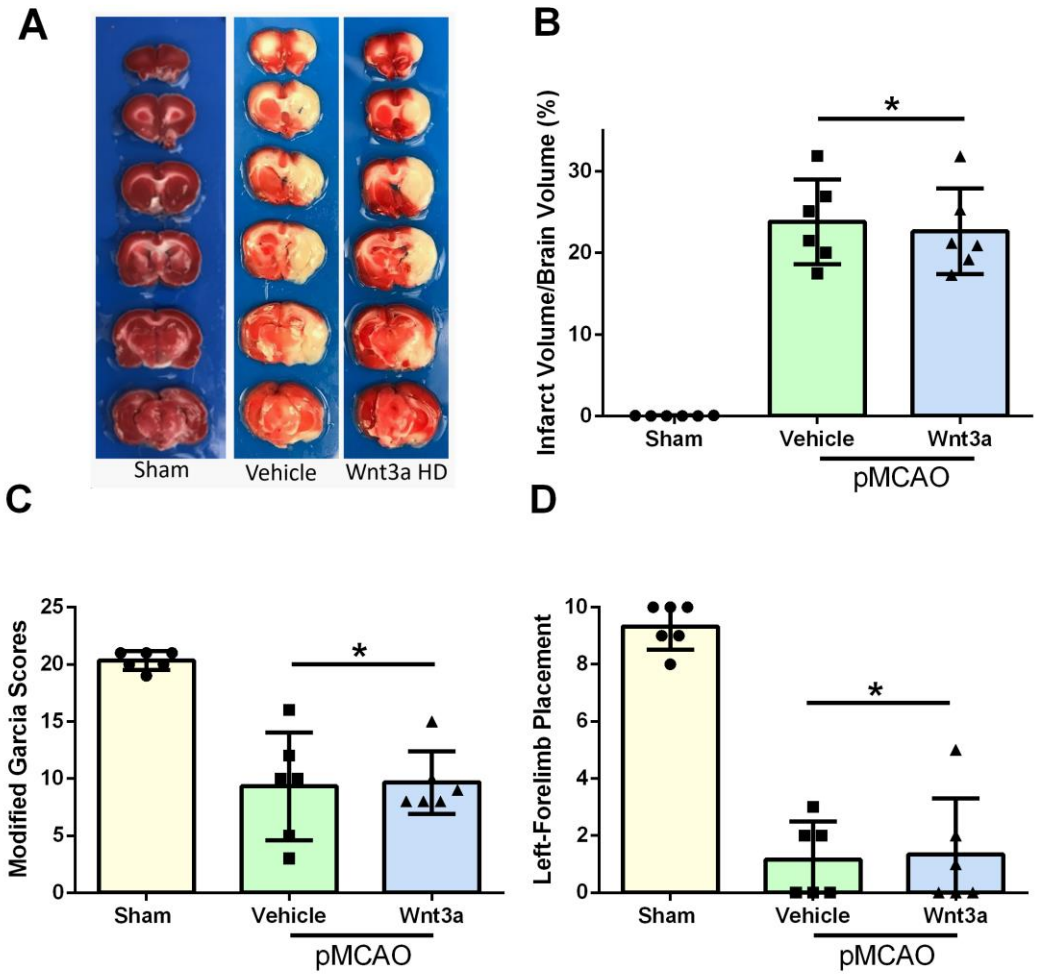

Figure 11. Infarct volumes 24 h post-pMCAO. (A) Representative TTC staining images of coronal sections. (B) Wnt3a HD had no effect on infarct in the pMCAO compared to vehicle. (C) Modified Garcia showed no improvement in neurological function after wnt3a administration. (D) Left-forelimb placement showed no improvement after wnt3a treatment compared to vehicle. Each column represents the mean ± SD (n=6/group). *p<0.05 vs. Sham, #p<0.05 vs vehicle.

Impact of Frz1-siRNA, PIWI1a-siRNA and PIWI CRISPR in Naïve Animals

Naïve animals were used to evaluate the effectiveness of siRNAs and CRISPR. NAÏVE+Frizzled siRNA significantly reduced Frizzled-1 protein levels compared to both NAÏVE and NAÏVE+Scrambled siRNA (One-way ANOVA; Tukey's test; $F(2, 15) = 34.15$; $n=6$, $p<0.05$; Fig 12A). In the Naïve+PIWI1a siRNA group, PIWI1a levels were significantly attenuated compared to NAÏVE and Naïve+Scrambled siRNA (One-way ANOVA; Tukey's test; $F(3, 20) = 24.51$; $n=6$, $p<0.05$; Fig 12B). This effect was reversed and restored to sham levels in the Naïve+PIWI1a CRISPR+Frz1siRNA group (One-way ANOVA; Tukey's test; $F(3, 20) = 34.15$; $n=6$, $p<0.05$; Fig 12B).

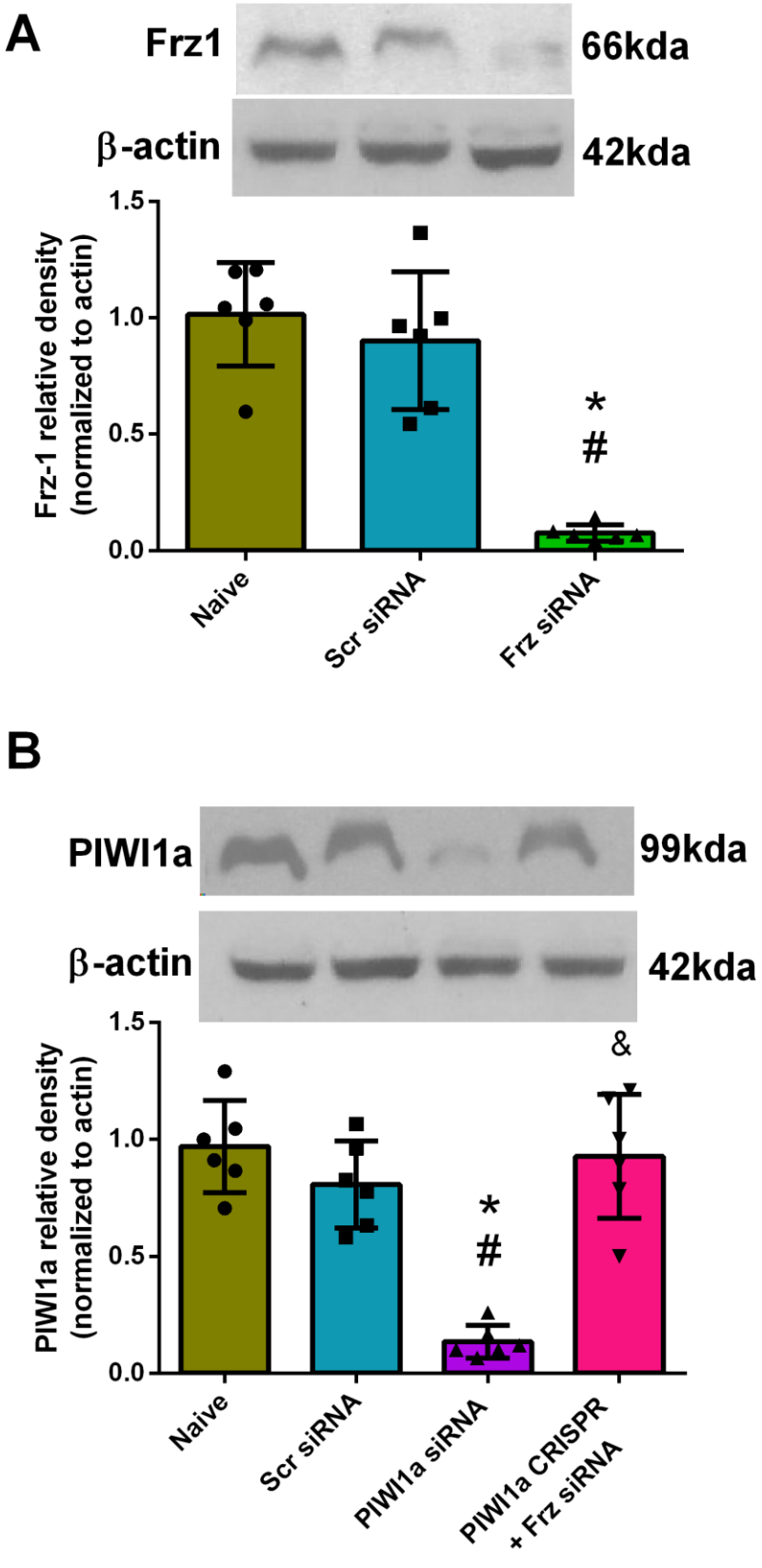
A
Frz1
66kda
β-actin
42kda
Frz-1 relative density
(normalized to actin)
1.5
1.0
0.5
0.0
*
#
Naive
Scr siRNA
Frz siRNA
B
PIWI1a
99kda
β-actin
42kda
PIWI1a relative density
(normalized to actin)
1.5
1.0
0.5
0.0
*
#
&
Naive
Scr siRNA
PIWI1a siRNA
PIWI1a CRISPR
+ Frz siRNA

Figure 12. Naïve treated animals showed a significant reduction of Frizzled-1 with Frz siRNA. (A) Representative western blots of the right hemisphere of the rat brain and quantitative analysis showed that the expression of Frizzled-1 significantly decreased at 24 hours after Frizzled-siRNA administration compared to Naïve and Naïve+Scrambled-siRNA ($p<0.05$). Each column represents the mean ± SD (n=6/group). *$p<0.05$ vs. Naive, #$p<0.05$ vs Naïve+Scrambled-siRNA.

Evaluation of Exogenous Recombinant wnt3a in Treated Animals

Since the recombinant mouse wnt3a (ab81484) protein was used for all molecular and behavioral studies, due to its homology to rat wnt3a, and could not be distinguished from the endogenously expressed wnt3a, a human recombinant wnt3a (ab 153563) protein with a specific tag was intranasally administered, 1.2 µg/kg, 1 h post recanalization to check delivery and presence of our drug. The human recombinant wnt3a protein was made by the parasite Schistosoma japonicum and had GST3 bound to the N-Terminus to distinguish it from proteins expressed by the rat. A specific GST antibody without binding affinity for the rat Glutathione S-transferase P protein (GSTP1 also known as GST3) was used to assess the amount of recombinant protein (ab153563) in our treated animals. Representative western blots and quantitative analysis showed that the amount of recombinant wnt3a GST-specific protein was significantly higher compared to non-treated groups, both sham and vehicle (One-way ANOVA; Tukey's test; $F(2, 15) = 285.4$; $n=6$, $p<0.05$; Fig 13A). Although exogenous delivery was confirmed in our study, further research is needed to thoroughly evaluate the pharmacokinetics of exogenous wnt3a administered after MCAO. Better pharmacokinetic understanding will be essential in the development of clinical applications and strengthening of wnt3a's translational impact.

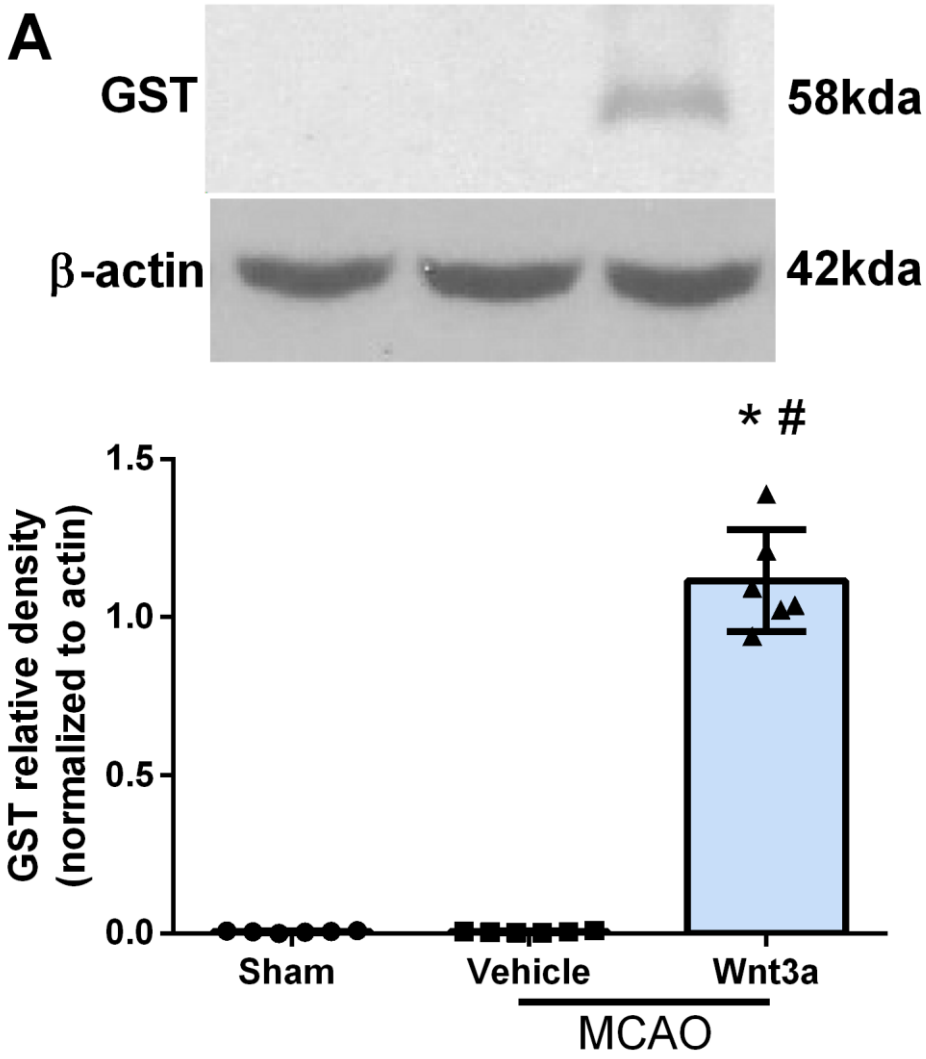

Figure 13. Western blot confirmed the delivery of wnt3a in our treated animals. (A) Right hemisphere representative Western blots of the rat brain and quantitative analysis showed that the expression of recombinant GST-specific tagged wnt3a protein was significantly higher compared to non-treated groups, both sham and vehicle. Each column represents the mean ± SD (n=6/group). *p<0.05 vs. Sham, #p<0.05 vs vehicle.

Wnt3a and Alternative Co-receptor LRP6 Binding

When wnt proteins bind to Frizzled cell surface receptors, the transmembrane lipoprotein receptor related proteins 5 and 6 (LRP5/6) are recruited, and, in the canonical wnt pathway, cytoplasmic protein Dishevelled (Dvl) is activated, which leads to the inhibition of GSK3 and prevention of the phosphorylation, degradation of β-catenin (Bhanot *et al.*, 1996; Abe *et al.*, 2013). Therefore, we further investigated the regulation of LRP6 after wnt3a treatment in MCAO. iN wnt3a (1.2 µg/kg) was administered at one hour after reperfusion in treatment groups, and western blot was performed on the right-hemisphere of the brain, representative images in Fig 14A. LRP6 levels were not significantly different between: sham, vehicle, MCAO+wnt3a, MCAO+wnt3a+scrambled-siRNA, and MCAO+wnt3a+Frz1-siRNA groups. However, the phosphorylated LRP6 levels were significantly higher in the HD (1.2 µg/kg) wnt3a groups compared to vehicle (One-way ANOVA; Tukey's test; $F(4, 25) = 17.76$; $n=6$, $p<0.05$; Fig 14A). This effect was reversed, significantly attenuating the pLRP6 expression in the MCAO+wnt3a+Frz1siRNA group compared to MCAO+wnt3a (One-way ANOVA; Tukey's test; $F(4, 25) = 17.76$; $n=6$, $p<0.05$; Fig 14A). This suggests that the phosphorylation of LRP6 is dependent on wnt3a-Frz1 binding, which is supported in literature-- wnt3a has a 2-3x stronger affinity towards Frz1 compared to LRP6 (Bourhis *et al.*, 2010). Phosphorylation of LRP6 may be responsible for additional regulation of GSK3 in our proposed neuronal pathway.

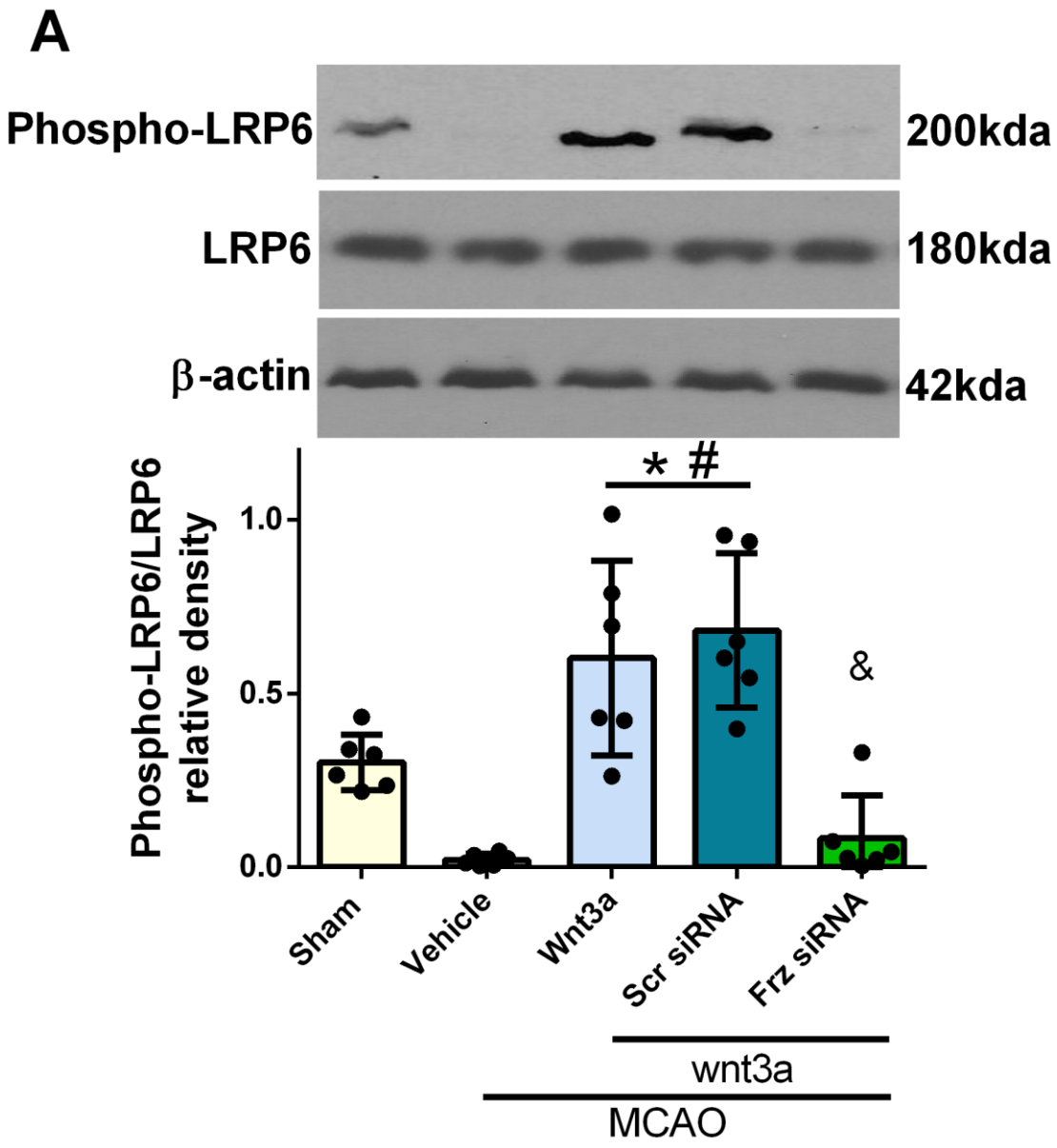

Figure 14. LRP6 expression and activation after MCAO in rats. (A) Right hemisphere representative Western blots of the rat brain for LRP6, pLRP6, and actin. Overall LRP6 (A) expression was not significant between groups. However, phosphorylation of LRP significantly increased in the HD treatment (1.2 μg/kg) treated groups, which was reversed in the Frz1-siRNA at 24HR after MCAO. Each column represents the mean ± SD (n=6/group). *p<0.05 vs. Sham, #p<0.05 vs vehicle, &p<0.05 vs. wnt3a + Scr siRNA.

Wnt3a Treatment Improved Long-term Neurobehavioral Outcome after MCAO

To evaluate the significance of wnt3a in attenuating long-term neurological deficits, we performed Morris water maze and rotarod tests at day 21 to 27 after MCAO. The three groups-- sham, vehicle, and wnt3a (HD)-- exhibited no significant difference in latency to escape onto the visible platform and swimming distances during the first day of visible platform tests (Fig. 12 A; One-way ANOVA; Tukey's test; n=8-12; $P>0.05$). For the hidden platform and the probe trials, rats in vehicle group did not learn to find the escape platform as rapidly, traveled longer distances, and spent less time in the target probe quadrants compared to sham (Fig. 12 A; One-way ANOVA; Tukey's test; n=8-12; $P<0.05$ vs Sham). Treatment with wnt3a significantly decreased the latency to find the platform, travel distance, and increased the time in the target quadrant compared to vehicle (Fig. 3A-C; One-way ANOVA; Tukey's test; n=6; $P<0.05$).

In the rotarod test, MCAO+vehicle rats had significantly impaired motor coordination compared to sham (Fig. 12 B; One-way ANOVA; Tukey's test; n=8-12; $P < 0.1$). Wnt3a improved performance in the 5 RPM and 10 RPM rotarod tests and restored performance to sham levels (Fig. 12 B).

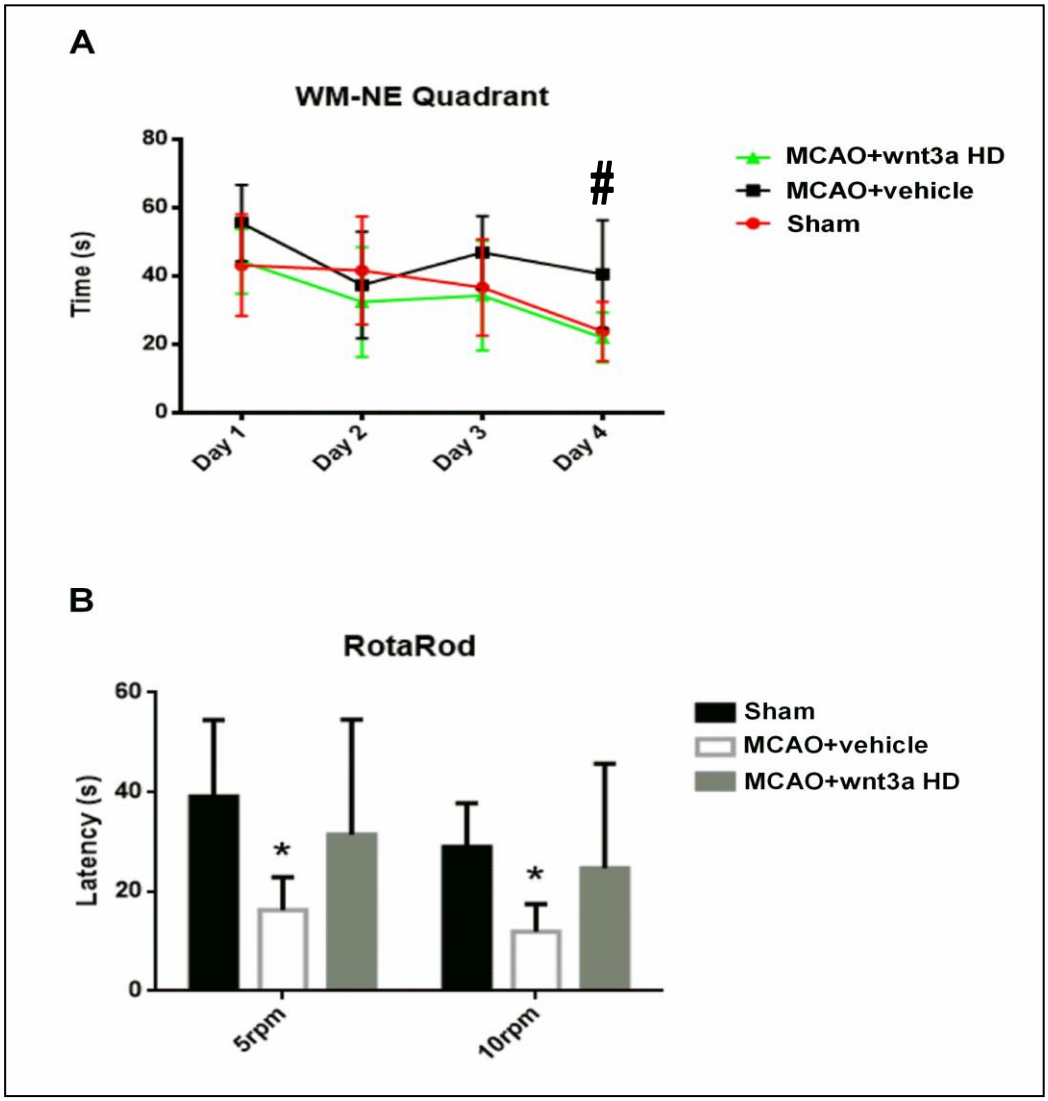

Figure 12. Watermaze data shows significance on day 4 (day24 from MCAO) for treatment compared to sham N=8-12/group, Mean ± SD, One-way ANOVA; # $p<0.05$ vs vehicle. For RotaRod, significance was observed in treatment with a *$p<0.1$vs Sham. N=8-12/group, Mean ± SD, One-way ANOVA

Discussion

In the present study, we made the following observations: (1) endogenous wnt3a and its downstream targets, Frz1/PIWI1a/FOXM1, were significantly decreased, while pGSK3β, and CC-3 were significantly increased in the brain at 24 h after MCAO; (2) intranasal wnt3a decreased infarct volume and improved neurobehavioral function at 24 h after MCAO; (3) immunofluorescence confirmed that neurons express the receptor of wnt3a, Frz1; (4) exogenous iN wnt3a administered one hour after MCAO significantly up-regulated the expression of Frz1, β-catenin, PIWI1a, and FOXM1 compared to vehicle groups and decreased CC-3 levels; (5) 72 h after MCAO, infarct size and neurobehavioral function improved after a single dose of wnt3a; (6) specific siRNAs showed links between Frz1, PIWI1a, and FOXM1 at 24 h after MCAO; (7) The same efficacy of wnt3a after stroke was seen in female rats, but the effect was diminished in aged rats; (8) In the pMCAO model, no significant difference was observed between vehicle and wnt3a groups.

Wnt3a caused significant increase in PIWI1a and FOXM1 and a decrease in CC-3 at 24 h after wnt3a administration. At 72 h, in the vehicle group, PIWI1a levels were restored to pre-stroke levels. This result suggests that either the modest recovery of endogenous wnt3a levels at 72 h or an alternate pathway is responsible for the upregulation of β-catenin, PIWI1a and FOXM1 levels 72 h after MCAO. In literature, although β-catenin expression was endogenously elevated at 72 h after SAH, neuronal survival was not significantly improved (Chen *et al.*, 2015), neuronal survival was not significantly improved. In this study, the higher β-catenin expression after wnt3a treatment significantly reduced apoptosis at 24 and 72 h endpoints.

To confirm that PIWI1a regulates FOXM1, a specific inhibitor of PIWI1a, PIWI1a-siRNA, was administered with wnt3a. This intervention caused a significant decrease in FOXM1 expression at 24 h. To further investigate the possibility of an alternative pathway, two groups were added: wnt3a+Frz1-siRNA+MCAO and wnt3a+Frz1-siRNA+PIWI1a-CRISPR-activation+MCAO. In the cohort of wnt3a+Frz1-siRNA+MCAO, we saw a significant reduction of PIWI1a and FOXM1; however in wnt3a+Frz1-siRNA+PIWI1a-CRISPR-activation+MCAO, PIWI1a levels were significantly increased with an associated increase in FOXM1 levels and a reduction in CC-3. These mechanistic studies support a link between PIWI1a and FOXM1.

Studies have shown a significant association between PIWIL1a and regulation of β-catenin (Reeves *et al.*, 2012), but PIWIL1a has not been mechanistically linked with wnt3a or downstream signaling after stroke. We found that PIWI1a significantly decreased the levels of active p-GSK3β and significantly rescued levels of survival protein β-catenin. Inhibition of PIWI1a significantly increased levels of p-GSK3β, suggesting that PIWI1a is an upstream regulator of GSK3β. A link between Frz1 and p-GSK3β is supported by increased p-GSK3β secondary to Frz1-siRNA. To confirm PIWI1a's role downstream of Frz1, PIWI1a was upregulated via CRISPR in combination with siRNA Frz1 knockdown. This upregulation of PIWI1a significantly down-regulated p-GSK3β.

Frz1 has been reportedly activated by wnt3a and shown to be neuroprotective against Aβ oligomers (Chacón *et al.*, 2008). We confirmed the presence of Frz1 in neurons using immunohistochemistry and noticed an increased expression of Frz1 in the penumbra of wnt3+MCAO compared to vehicle+MCAO group. Western blots also

supported that iN administration of wnt3a significantly increased the expression of Frz1 at 24 and 72 h. These findings suggest a positive feedback loop involving wnt3a and Frz1. Additionally, the inhibition of PIWI1a with siRNA resulted in decreased expression of Frz1, indicating that Frz1 may be transcriptionally regulated downstream of PIWI1a. Congruently, the canonical wnt3a/Frz1 pathway in cancer tissues significantly decreased certain miRNAs (eg. miR-204 for Frz1) which may be a variable in the increased expression of the Frz1 receptor (Ueno *et al.*, 2013). The Frz1 positive-feedback loop requires further investigation. Inhibition of Frz1 down-regulated wnt3a, PIWI1a, β-catenin, and FOXM1, while upregulating p-GSK3β and CC-3 expression at 24h.

Interestingly, wnt3a protein expression was significantly reduced in the Frz1-siRNA group. In support of this finding, miR-34 was observed to directly attenuate wnt3a protein expression in breast cancer tissues (Song *et al.*, 2015). Additionally, in gastric carcinoma cells, TGF-β induces caspase-8 activation and apoptosis by phosphorylating R-Smads-- which form complexes with their common mediator, Smad4, and enter the nucleus to regulate gene expression (Moustakas & Heldin, 2005). This Smad-complex has been shown to attenuate the wnt expression in cancer cell lines (Tian *et al.*, 2009; Voorneveld *et al.*, 2015). A potential upstream link exists via the ability of GSK3β to phosphorylate and activate Smad4 to lower the expression of wnt3a, an effect which is reversed after wnt3a treatment in HEK cells (Demagny *et al.*, 2014). Despite several promising hypotheses, further research is needed to elucidate the gene regulation of wnt3a after Frz1 siRNA treatment in neurons after MCAO in the rat model. Although

these limitations, we can conclude that wnt3a exerts neuroprotective effects on PIWI1a/β-catenin/FOXM1 through the Frz1 receptor.

In the present study, we investigated two pro-apoptotic proteins, pGSK3β and CC-3. GSK-3β is reported to participate in neuron death through PI3K/AKT and wnt/β-catenin signaling pathways after stroke (Chen *et al.*, 2016). Also, after MCAO, CC-3 significantly increased and caused apoptosis in neurons (Li *et al.*, 2017). Paralleling these findings, we observed an increase in pGSK3β and CC-3 at 24h and 72h after MCAO. These effects were directly reversed with iN wnt3a treatment. This reduction in neuronal apoptotic proteins with wnt3a administration was associated with significant neurobehavior improvement in forelimb placement and recovery of Modified Garcia scores to sham levels. Studies have shown that MCAO causes deleterious neurological effects on Modified Garcia (Wang *et al.*, 2017), and left fore-limb placement (Senda *et al.*, 2011), tests that correlate the cerebral infarction. We examined the neuropathological damage at 24 and 72 h after MCAO and found our model to create significant neurological deficits. Wnt3a had a significant reduction of infarction volumes and neurological deficits in female rats. Efficacy of wnt3a diminished with age, but significant benefits were seen in both infarct volume and fore-limb placement. In a permanent occlusion model, there was no change after wnt3a administration in infarct volume and neurological outcome. This may be due to lack of wnt3a flow to the infarcted core. The proposed mechanism of action of wnt3a requires interaction of wnt3a with receptors, and thus direct sanguineous exposure to the area of infarction is likely required for therapeutic effect. While the penumbra of the infarction zone receives some perfusion and thus wnt3a exposure in models of permanent occlusion, without reperfusion, there is

limited opportunity for rescue of severely hypoxic penumbra. In agreement with our findings, a significant number of proposed neuroprotective agents have only demonstrated effectiveness in animal models of transient occlusion (Min *et al.*, 2013). Behavior was restored to sham levels after low dose wnt3a and high dose wnt3a administration in the following neurological tests: modified Garcia, left forelimb placement, and corner turn. In vehicle groups, performance was significantly worse in all groups compared to sham. When compared to treated groups significance was only seen on left-forelimb placement tests. This coincides with previous research that infarct volume affects neurobehavior tests, but sometimes these tests are not as sensitive to evaluate the total damage in the pathology of stroke since each test is only sensitive to specific focal neurological deficits (Senda *et al.*, 2011); nonetheless, this treatment shows promise in improving the neurobehavioral rehabilitation of patients.

Due to the filtering nature of the blood brain barrier (BBB), treatments targeting the central nervous system (CNS) that are administered outside of the CNS must be able to efficiently cross the BBB (Thorne & Frey, 2001). iN administration of neuroprotectants has previously been established as a viable route of administration for stroke with the benefit allowing rapid delivery to the CNS and ease of administration (Lin *et al.*, 2009). We found that wnt3a's delivery via an iN route was feasible and provided neuroprotection after stroke. Thus, iN administration of wnt3a is a clinically translatable route of administration, lowering risk of systemic side-effects caused by other less desirable routes of administration.

One limitation of this study is that the design and results do not fully exclude the possibility of alternative pathways that act on wnt3a and downstream mediators; thus,

further research will need to investigate the relationship between PIWI1a, β-catenin, FOXM1, and the canonical apoptosis pathway to fully exclude or incorporate alternative pathways that may play a role in wnt3a physiology. For example, β-catenin canonically is known to translocate into the nucleus and act as a transcriptional coactivator of transcription factors that belong to the TCF/LEF family (Rao & Kühl, 2010). Wnt3a is known to bind to Frz1a, expressed by dendrites (Oderup *et al.*, 2013) and microglia, which may play a role in the regulation of apoptosis in neurons. Additionally, GSK3β is part of the destruction complex (APC, Axin, and CK1) (Minde *et al.*, 2011) of β-catenin and can be regulated by these intrinsic proteins, a process in which PIWIL1a may be a significant player. Further mechanistic studies of these three proteins independently needs to be investigated to fully understand the role of PIWIl1a in the wnt3a pathway.

In conclusion, intranasal administration of wnt3a was efficacious in neuroprotection against transient cerebral ischemia in rats. New pathway links between Frz1, PIWI1a, and FOXM1 have been established by which wnt3a works in neurons to inhibit caspase-3 dependent apoptosis. A working model of these relationships is shown in Fig 1. Given the lack of treatment options for ischemic brain injury after stroke, these findings provide a basis for clinical trials to advance the clinical management of stroke and a foundation for future research in similar pathologies. Wnt3a intranasal delivery should be investigated further as a potential therapeutic option for ischemic stroke.

References

Abe, T., Zhou, P., Jackman, K., Capone, C., Casolla, B., Hochrainer, K., Kahles, T., Ross, M.E., Anrather, J., & Iadecola, C. (2013) Lipoprotein Receptor–Related Protein-6 Protects the Brain From Ischemic Injury. *Stroke*, **44**, 2284–2291.

Arrázola, M.S., Silva-Alvarez, C., & Inestrosa, N.C. (2015) How the Wnt signaling pathway protects from neurodegeneration: the mitochondrial scenario. *Front. Cell. Neurosci.*, **9**.

Ayer, R.E., Jafarian, N., Chen, W., Applegate, R.L., Colohan, A.R.T., & Zhang, J.H. (2012) Preoperative mucosal tolerance to brain antigens and a neuroprotective immune response following surgical brain injury. *J. Neurosurg.*, **116**, 246–253.

Bhanot, P., Brink, M., Samos, C.H., Hsieh, J.C., Wang, Y., Macke, J.P., Andrew, D., Nathans, J., & Nusse, R. (1996) A new member of the frizzled family from Drosophila functions as a Wingless receptor. *Nature*, **382**, 225–230.

Bortesi, L. & Fischer, R. (2015) The CRISPR/Cas9 system for plant genome editing and beyond. *Biotechnol. Adv.*, **33**, 41–52.

Bourhis, E., Tam, C., Franke, Y., Bazan, J.F., Ernst, J., Hwang, J., Costa, M., Cochran, A.G., & Hannoush, R.N. (2010) Reconstitution of a frizzled8.Wnt3a.LRP6 signaling complex reveals multiple Wnt and Dkk1 binding sites on LRP6. *J. Biol. Chem.*, **285**, 9172–9179.

Candelario-Jalil, E. (2009) Injury and repair mechanisms in ischemic stroke: considerations for the development of novel neurotherapeutics. *Curr. Opin. Investig. Drugs Lond. Engl. 2000*, **10**, 644–654.

Cerpa, W., Toledo, E.M., Varela-Nallar, L., & Inestrosa, N.C. (2009) The role of Wnt signaling in neuroprotection. *Drug News Perspect.*, **22**, 579–591.

Chacón, M.A., Varela-Nallar, L., & Inestrosa, N.C. (2008) Frizzled-1 is involved in the neuroprotective effect of Wnt3a against Abeta oligomers. *J. Cell. Physiol.*, **217**, 215–227.

Chen, C., Ostrowski, R.P., Zhou, C., Tang, J., & Zhang, J.H. (2010) Suppression of hypoxia-inducible factor-1alpha and its downstream genes reduces acute hyperglycemia-enhanced hemorrhagic transformation in a rat model of cerebral ischemia. *J. Neurosci. Res.*, **88**, 2046–2055.

Chen, S., Ma, Q., Krafft, P.R., Hu, Q., Rolland, W., Sherchan, P., Zhang, J., Tang, J., & Zhang, J.H. (2013) P2X7R/cryopyrin inflammasome axis inhibition reduces neuroinflammation after SAH. *Neurobiol. Dis.*, **58**, 296–307.

Chen, W., Ma, Q., Suzuki, H., Hartman, R., Tang, J., & Zhang, J.H. (2011) Osteopontin reduced hypoxia-ischemia neonatal brain injury by suppression of apoptosis in a rat pup model. *Stroke J. Cereb. Circ.*, **42**, 764–769.

Chen, X., Liu, Y., Zhu, J., Lei, S., Dong, Y., Li, L., Jiang, B., Tan, L., Wu, J., Yu, S., & Zhao, Y. (2016) GSK-3β downregulates Nrf2 in cultured cortical neurons and in a rat model of cerebral ischemia-reperfusion. *Sci. Rep.*, **6**.

Chen, Y., Zhang, Y., Tang, J., Liu, F., Hu, Q., Luo, C., Tang, J., Feng, H., & Zhang, J.H. (2015) Norrin protected blood-brain barrier via frizzled-4/β-catenin pathway after subarachnoid hemorrhage in rats. *Stroke*, **46**, 529–536.

Cohen, P. & Goedert, M. (2004) GSK3 inhibitors: development and therapeutic potential. *Nat. Rev. Drug Discov.*, **3**, 479–487.

Collino, M., Aragno, M., Castiglia, S., Tomasinelli, C., Thiemermann, C., Boccuzzi, G., & Fantozzi, R. (2009) Insulin Reduces Cerebral Ischemia/Reperfusion Injury in the Hippocampus of Diabetic Rats. *Diabetes*, **58**, 235–242.

Demagny, H., Araki, T., & De Robertis, E.M. (2014) The Tumor Suppressor Smad4/DPC4 Is Regulated by Phosphorylations that Integrate FGF, Wnt, and TGF-β Signaling. *Cell Rep.*, **9**, 688–700.

Ferrer, I. & Planas, A.M. (2003) Signaling of cell death and cell survival following focal cerebral ischemia: life and death struggle in the penumbra. *J. Neuropathol. Exp. Neurol.*, **62**, 329–339.

Fisher, M. & Brott, T.G. (2003) Emerging Therapies for Acute Ischemic Stroke New Therapies on Trial. *Stroke*, **34**, 359–361.

Freeman, T.J., Smith, J.J., Chen, X., Washington, M.K., Roland, J.T., Means, A.L., Eschrich, S.A., Yeatman, T.J., Deane, N.G., & Beauchamp, R.D. (2012) Smad4-Mediated Signaling Inhibits Intestinal Neoplasia by Inhibiting Expression of β-Catenin. *Gastroenterology*, **142**, 562–571.e2.

Gratz, S.J., Cummings, A.M., Nguyen, J.N., Hamm, D.C., Donohue, L.K., Harrison, M.M., Wildonger, J., & O'Connor-Giles, K.M. (2013) Genome Engineering of Drosophila with the CRISPR RNA-Guided Cas9 Nuclease. *Genetics*, **194**, 1029–1035.

Horvath, P. & Barrangou, R. (2010) CRISPR/Cas, the Immune System of Bacteria and Archaea. *Science*, **327**, 167–170.

Hu, Q., Chen, C., Yan, J., Yang, X., Shi, X., Zhao, J., Lei, J., Yang, L., Wang, K., Chen, L., Huang, H., Han, J., Zhang, J.H., & Zhou, C. (2009) Therapeutic application of gene silencing MMP-9 in a middle cerebral artery occlusion-induced focal ischemia rat model. *Exp. Neurol.*, **216**, 35–46.

Inestrosa, N.C. & Varela-Nallar, L. (2014) Wnt signaling in the nervous system and in Alzheimer's disease. *J. Mol. Cell Biol.*, **6**, 64–74.

Jiang, L., Wang, P., Chen, L., & Chen, H. (2014) Down-regulation of FoxM1 by thiostrepton or small interfering RNA inhibits proliferation, transformation ability and angiogenesis, and induces apoptosis of nasopharyngeal carcinoma cells. *Int. J. Clin. Exp. Pathol.*, **7**, 5450–5460.

Jiang, W., Bikard, D., Cox, D., Zhang, F., & Marraffini, L.A. (2013) RNA-guided editing of bacterial genomes using CRISPR-Cas systems. *Nat. Biotechnol.*, **31**, 233.

Jinek, M., Chylinski, K., Fonfara, I., Hauer, M., Doudna, J.A., & Charpentier, E. (2012) A programmable dual-RNA-guided DNA endonuclease in adaptive bacterial immunity. *Science*, **337**, 816–821.

Kelly, S., Zhao, H., Hua Sun, G., Cheng, D., Qiao, Y., Luo, J., Martin, K., Steinberg, G.K., Harrison, S.D., & Yenari, M.A. (2004) Glycogen synthase kinase 3β inhibitor Chir025 reduces neuronal death resulting from oxygen-glucose deprivation, glutamate excitotoxicity, and cerebral ischemia. *Exp. Neurol.*, **188**, 378–386.

Kusaka, I., Kusaka, G., Zhou, C., Ishikawa, M., Nanda, A., Granger, D.N., Zhang, J.H., & Tang, J. (2004) Role of AT1 receptors and NAD(P)H oxidase in diabetes-aggravated ischemic brain injury. *Am. J. Physiol. Heart Circ. Physiol.*, **286**, H2442-2451.

Lai, T.W., Zhang, S., & Wang, Y.T. (2014) Excitotoxicity and stroke: Identifying novel targets for neuroprotection. *Prog. Neurobiol.*, 2013 Pangu Meeting on Neurobiology of Stroke and CNS Injury: Progresses and Perspectives of Future, **115**, 157–188.

Li, C., Che, L.-H., Ji, T.-F., Shi, L., & Yu, J.-L. (2017) Effects of the TLR4 signaling pathway on apoptosis of neuronal cells in diabetes mellitus complicated with cerebral infarction in a rat model. *Sci. Rep.*, **7**, srep43834.

Lin, S., Fan, L.-W., Rhodes, P.G., & Cai, Z. (2009) Intranasal administration of IGF-1 attenuates hypoxic-ischemic brain injury in neonatal rats. *Exp. Neurol.*, **217**, 361–370.

Liu, L., Puri, K.D., Penninger, J.M., & Kubes, P. (2007) Leukocyte PI3Kgamma and PI3Kdelta have temporally distinct roles for leukocyte recruitment in vivo. *Blood*, **110**, 1191–1198.

Liu, X.F., Fawcett, J.R., Thorne, R.G., DeFor, T.A., & Frey, W.H. (2001) Intranasal administration of insulin-like growth factor-I bypasses the blood-brain barrier and protects against focal cerebral ischemic damage. *J. Neurol. Sci.*, **187**, 91–97.

Ma, Y.-P., Ma, M.-M., Cheng, S.-M., Ma, H.-H., Yi, X.-M., Xu, G.-L., & Liu, X.-F. (2008) Intranasal bFGF-induced progenitor cell proliferation and neuroprotection after transient focal cerebral ischemia. *Neurosci. Lett.*, **437**, 93–97.

MacDonald, B.T., Tamai, K., & He, X. (2009) Wnt/β-catenin signaling: components, mechanisms, and diseases. *Dev. Cell*, **17**, 9–26.

Mackay, J. & Mensah, G. (2004) *Atlas of Heart Disease and Stroke*, 1 edition. edn. World Health Organization, Geneva.

Mali, P., Yang, L., Esvelt, K.M., Aach, J., Guell, M., DiCarlo, J.E., Norville, J.E., & Church, G.M. (2013) RNA-Guided Human Genome Engineering via Cas9. *Science*, **339**, 823–826.

McBride, D.W., Tang, J., & Zhang, J.H. (2016) Development of an Infarct Volume Algorithm to Correct for Brain Swelling After Ischemic Stroke in Rats. *Acta Neurochir. Suppl.*, **121**, 103–109.

Minde, D.P., Anvarian, Z., Rüdiger, S.G., & Maurice, M.M. (2011) Messing up disorder: how do missense mutations in the tumor suppressor protein APC lead to cancer? *Mol. Cancer*, **10**, 101.

Molina, C.A. & Saver, J.L. (2005) Extending reperfusion therapy for acute ischemic stroke: emerging pharmacological, mechanical, and imaging strategies. *Stroke J. Cereb. Circ.*, **36**, 2311–2320.

Moustakas, A. & Heldin, C.-H. (2005) Non-Smad TGF-β signals. *J Cell Sci*, **118**, 3573–3584.

Oderup, C., LaJevic, M., & Butcher, E.C. (2013) Canonical and non-canonical Wnt proteins program dendritic cell responses for tolerance. *J. Immunol. Baltim. Md 1950*, **190**, 6126–6134.

Pang, L., Qiu, T., Cao, X., & Wan, M. (2011) Apoptotic role of TGF-β mediated by Smad4 mitochondria translocation and cytochrome c oxidase subunit II interaction. *Exp. Cell Res.*, **317**, 1608–1620.

Perez-Pinera, P., Kocak, D.D., Vockley, C.M., Adler, A.F., Kabadi, A.M., Polstein, L.R., Thakore, P.I., Glass, K.A., Ousterout, D.G., Leong, K.W., Guilak, F., Crawford, G.E., Reddy, T.E., & Gersbach, C.A. (2013) RNA-guided gene activation by CRISPR-Cas9-based transcription factors. *Nat. Methods*, **10**, 973–976.

Petty, M.A. & Lo, E.H. (2002) Junctional complexes of the blood-brain barrier: permeability changes in neuroinflammation. *Prog. Neurobiol.*, **68**, 311–323.

Rao, T.P. & Kühl, M. (2010) An Updated Overview on Wnt Signaling Pathways A Prelude for More. *Circ. Res.*, **106**, 1798–1806.

Reeves, M.E., Baldwin, M.L., Aragon, R., Baldwin, S., Chen, S.-T., Li, X., Mohan, S., & Amaar, Y.G. (2012) RASSF1C modulates the expression of a stem cell renewal gene, PIWIL1. *BMC Res. Notes*, **5**, 239.

Rha, J.-H. & Saver, J.L. (2007) The Impact of Recanalization on Ischemic Stroke Outcome: A Meta-Analysis. *Stroke*, **38**, 967–973.

Roth, J.M. (2011) Recombinant tissue plasminogen activator for the treatment of acute ischemic stroke. *Proc. Bayl. Univ. Med. Cent.*, **24**, 257–259.

Schmued, L.C., Stowers, C.C., Scallet, A.C., & Xu, L. (2005) Fluoro-Jade C results in ultra high resolution and contrast labeling of degenerating neurons. *Brain Res.*, **1035**, 24–31.

Senda, D.M., Franzin, S., Mori, M.A., de Oliveira, R.M.W., & Milani, H. (2011) Acute, post-ischemic sensorimotor deficits correlate positively with infarct size but fail to predict its occurrence and magnitude after middle cerebral artery occlusion in rats. *Behav. Brain Res.*, **216**, 29–35.

Shruster, A., Ben-Zur, T., Melamed, E., & Offen, D. (2012) Wnt signaling enhances neurogenesis and improves neurological function after focal ischemic injury. *PloS One*, **7**, e40843.

Song, J.L., Nigam, P., Tektas, S.S., & Selva, E. (2015) microRNA regulation of Wnt signaling pathways in development and disease. *Cell. Signal.*, **27**, 1380–1391.

Thorne, R.G., Emory, C.R., Ala, T.A., & Frey, W.H. (1995) Quantitative analysis of the olfactory pathway for drug delivery to the brain. *Brain Res.*, **692**, 278–282.

Thorne, R.G. & Frey, W.H. (2001) Delivery of neurotrophic factors to the central nervous system: pharmacokinetic considerations. *Clin. Pharmacokinet.*, **40**, 907–946.

Tian, X., Du, H., Fu, X., Li, K., Li, A., & Zhang, Y. (2009) Smad4 restoration leads to a suppression of Wnt/β-catenin signaling activity and migration capacity in human colon carcinoma cells. *Biochem. Biophys. Res. Commun.*, **380**, 478–483.

Ueno, K., Hirata, H., Hinoda, Y., & Dahiya, R. (2013) Frizzled homolog proteins, microRNAs and Wnt Signaling in Cancer. *Int. J. Cancer J. Int. Cancer*, **132**, 1731–1740.

Voorneveld, P.W., Kodach, L.L., Jacobs, R.J., van Noesel, C.J.M., Peppelenbosch, M.P., Korkmaz, K.S., Molendijk, I., Dekker, E., Morreau, H., van Pelt, G.W., Tollenaar, R. a. E.M., Mesker, W., Hawinkels, L.J. a. C., Paauwe, M., Verspaget, H.W., Geraets, D.T., Hommes, D.W., Offerhaus, G.J.A., van den Brink, G.R., ten Dijke, P., & Hardwick, J.C.H. (2015) The BMP pathway either enhances or inhibits the

Wnt pathway depending on the SMAD4 and p53 status in CRC. *Br. J. Cancer*, **112**, 122–130.

Wang, Y., Sherchan, P., Huang, L., Akyol, O., McBride, D.W., & Zhang, J.H. (2017) Naja sputatrix Venom Preconditioning Attenuates Neuroinflammation in a Rat Model of Surgical Brain Injury via PLA2/5-LOX/LTB4 Cascade Activation. *Sci. Rep.*, **7**, 5466.

Wnt Receptors & Pathways: R&D Systems [WWW Document] (2018) . URL https://www.rndsystems.com/resources/articles/wnt-receptors-pathways

Wu, X., Deng, G., Hao, X., Li, Y., Zeng, J., Ma, C., He, Y., Liu, X., & Wang, Y. (2014) A Caspase-Dependent Pathway Is Involved in Wnt/β-Catenin Signaling Promoted Apoptosis in Bacillus Calmette-Guerin Infected RAW264.7 Macrophages. *Int. J. Mol. Sci.*, **15**, 5045–5062.

Zhang, N., Wei, P., Gong, A., Chiu, W.-T., Lee, H.-T., Colman, H., Huang, H., Xue, J., Liu, M., Wang, Y., Sawaya, R., Xie, K., Yung, W.K.A., Medema, R.H., He, X., & Huang, S. (2011) FoxM1 promotes β-catenin nuclear localization and controls Wnt target-gene expression and glioma tumorigenesis. *Cancer Cell*, **20**, 427–442.

Zhao, Y., Wei, Z.Z., Zhang, J.Y., Zhang, Y., Won, S., Sun, J., Yu, S.P., Li, J., & Wei, L. (2017) GSK-3β Inhibition Induced Neuroprotection, Regeneration, and Functional Recovery After Intracerebral Hemorrhagic Stroke. *Cell Transplant.*, **26**, 395–407.

CHAPTER THREE

DISCUSSION

Nathanael Matei[1]

Department of [1]Physiology, Loma Linda University, Loma Linda, California 92354

Note: Most of this chapter is taken from a review paper currently in the submission process

Discussion

The glycolipoprotein hormone wnt3a is highly innovative as a therapy in the pathophysiology of stroke. Although the canonical wnt pathway has been extensively investigated, the identification of new isoforms of wnt and their unique mechanistic endpoints has revived therapeutic interest in wnt (Cerpa *et al.*, 2009; Shruster *et al.*, 2012; Inestrosa & Varela-Nallar, 2014). Therefore, wnt3a has potential as a neuroprotective therapy after stroke. As mentioned before, a mouse model was recently used to look at focal brain ischemia, induced by 1µl of the vasoconstrictor endothelial-1 and descriptively reported that wnt3a can produce significant neurogenesis (Shruster et al., 2012), but an improved model, such as MCAO, was needed to assess the immediate apoptotic implications and clinically translatable impact of wnt3a in a long-term study. The intracellular pathway by which wnt3a mediates its effects in neurons was poorly understood. Our study proposed a working model of the pathway for wnt3a in neurons. Specifically, wnt3a binds to Frz1, increasing PIWI1a, which inhibits the activation GSK3β and activates β-catenin, and translocates into the nucleus to increase the transcription of FOXM1—a survival protein that inhibits apoptosis. We believe that the recent discovery of new immune and apoptotic modulating functions for wnt3a, along with an incompletely detailed mechanism, especially in the stroke model, makes wnt3a an innovative candidate for treatment of stroke.

Currently, only 5% of patients receive rTPA to recanalize the blood vessel after stroke. No current therapy is given to help neuroprotection and promote neuronal cell survival in stroke. Due to the significance in our findings, wnt3a shows promise in preventing neuronal apoptosis. Given the lack of treatment options for ischemic brain

injury after stroke, this dissertation, if substantiated, may change the clinical management of stroke patients and provide a foundation for future research in other types of strokes with similar pathologies.

Translational Impact for Advancement of the Field

In 2015, several landmark clinical trials comparing the efficacy pharmacological and mechanical thrombectomy for treatment of large vessel ischemic stroke were published (Goyal et al., 2016). These studies support mechanical thrombectomy as the standard of care for rapidly diagnosed large vessel stroke. Given the results of these studies, networks of care will continue optimization to maximize the fraction of patients presenting within the appropriate time window to receive pharmacological thrombectomy, and when available, mechanical thrombectomy. Furthermore, recent trials have extended the eligible time window for reperfusion to 16 hours and beyond given appropriate magnetic resonance imaging selection criteria (Leslie-Mazwi et al., 2016; Albers et al., 2018). These findings have significant translational relevance to our findings in animal models of stroke. Wnt3a treatment showed limited efficacy in permanent occlusion, but promising reduction in infarction volume and improvement in neurobehavioral outcomes in the context of reperfusion. In the clinical context, wnt3a would thus best be applied in patients eligible for pharmacological or mechanical thrombectomy. Increasingly more patients will be screened with early magnetic resonance imaging to identify patients with adequate collateral blood supply allowing for delayed rescue of the penumbra (Jovin et al., 2017). These patients will be ideal candidates for therapies such as wnt3a that pair optimally with reperfusion.

Clinical research has established the principle of "time is brain," meaning that time delay before intervention is proportional to the loss of brain tissue (Saver, 2006). This principle emphasizes the need for early intervention in stroke, especially in patients with poor collateral blood supply. In practice, this requires that the planned intervention be feasible and easily deployed in the field. Although further research is needed to understand the pharmacokinetics and develop optimum dosing schedules, intranasal administration of wnt3a would theoretically allow rapid deployment following positive findings on computed tomography screening or even administration by emergency response personnel in cases of high pre-test probability of ischemic stroke.

The magnitude of stroke incidence justifies further investigation of interventions with potential for notable effect sizes (Rahlfs et al., 2014). Even small improvements in treatment of ischemic stroke will, nonetheless, have profound effects at the level of populations. Balancing the effect size of wnt3a intervention against the absence of observed side-effects in our animal models, wnt3a is a promising candidate for translation and has strong potential to advance the field of stroke therapy in combination with recent advancements in reperfusion therapy.

References

Albers GW et al. (2018) Thrombectomy for Stroke at 6 to 16 Hours with Selection by Perfusion Imaging. N Engl J Med 378:708–718.

Cerpa W, Toledo EM, Varela-Nallar L, Inestrosa NC (2009) The role of Wnt signaling in neuroprotection. Drug News Perspect 22:579–591.

Goyal M et al. (2016) Endovascular thrombectomy after large-vessel ischaemic stroke: a meta-analysis of individual patient data from five randomised trials. Lancet Lond Engl 387:1723–1731.

Inestrosa NC, Varela-Nallar L (2014) Wnt signaling in the nervous system and in Alzheimer's disease. J Mol Cell Biol 6:64–74.

Jovin TG et al. (2017) Diffusion-weighted imaging or computerized tomography perfusion assessment with clinical mismatch in the triage of wake up and late presenting strokes undergoing neurointervention with Trevo (DAWN) trial methods. Int J Stroke 12:641–652.

Leslie-Mazwi TM, Hirsch JA, Falcone GJ, Schaefer PW, Lev MH, Rabinov JD, Rost NS, Schwamm L, González RG (2016) Endovascular Stroke Treatment Outcomes After Patient Selection Based on Magnetic Resonance Imaging and Clinical Criteria. JAMA Neurol 73:43.

Rahlfs VW, Zimmermann H, Lees KR (2014) Effect Size Measures and Their Relationships in Stroke Studies. Stroke 45:627–633.

Saver JL (2006) Time is brain--quantified. Stroke 37:263–266.

Shruster A, Ben-Zur T, Melamed E, Offen D (2012) Wnt signaling enhances neurogenesis and improves neurological function after focal ischemic injury. PloS One 7:e40843.